Table 3

Summary of genetic variations of *CES1A1* and *var 1A1* exon 1s and their flanking regions detected in this study

SNP identification				Position					
This study	NCBI (dbSNP)	JSNP	Location	NT_010498.15	From the translational initiation site or the nearest exon	Nucleotide change and flanking sequences (5′ to 3′)	Amino acid change	Allele frequency (n = 354)*	*CES1A1* variant (*CES1A2* type)
MPJ6_CS1001†			5′-flank	9481424	–258	ttgggcaagtttacagctct**C/T**tgtaatctgacagtagagtc		0.014	
MPJ6_CS1002†			5′-flank	9481399	–233	atctgacagtagagtccaga**C/A**tggtttgatgaaagagggta		0.003	
MPJ6_CS1003†			5′-flank	9481327	–161	tagaagcccagggagatctg**A/G**ggaaagggagggcttttctg		0.006	
MPJ6_CS1004	rs3815583	IMS-JST175949	Exon1(5′-UTR)	9481241	–75	aactctgggcggggctgggc**G/T**ccagggctggacagcacagt		0.41	
MPJ6_CS1005	rs28429139		Exon1(5′-UTR)	9481212	–46	ggacagcacagtccctctga**A/G**ctgcacagagacctcgcagg		0.299	*var1A1*
MPJ6_CS1006	rs28494177		Exon1(5′-UTR)	9481205	–39	acagtccctctgaactgcac**A/G**gagacctcgcaggccccgag		0.299	*var1A1*
MPJ6_CS1007†			Exon1(5′-UTR)	9481196	–30	ctgaactgcacagagacctc**G/A**caggccccgagaactgtcgc		0.042	
MPJ6_CS1008	rs28520463		Exon1(5′-UTR)	9481187	–21	acagagacctcgcaggccccc**G/C**agaactgtcgcccttccacg		0.297	*var1A1*
MPJ6_CS1009	rs28499065		Exon1(5′-UTR)	9481186	–20	cagagacctcgcaggccccg**A/G**gaactgtcgcccttccacga		0.297	*var1A1*
MPJ6_CS1010	rs28515828		Exon1(5′-UTR)	9481168	–2	cgagaactgtcgcccttccac**C/G**gatgtggctccgtgcctttta		0.299	*var1A1*
MPJ6_CS1011			Exon 1	9481156	11	cccttccacgatgtggctcc**G/C**tgcctttatcctggccactc	Arg4Pro	0.297	*var1A1*
MPJ6_CS1012			Exon 1	9481152	15	tccacgatgtggctccgtgc**C/T**tttatcctggccactctctc	Ala5Ala	0.297	*var1A1*
MPJ6_CS1013			Exon 1	9481151	16	ccacgatgtggctccgtgcc**T/C**ttatcctggccactctctct	Phe6Leu	0.297	*var1A1*
MPJ6_CS1014			Exon 1	9481148	19	cgatgtggctccgtgcctttt**A/G**tcctggccactctctctgct	Ile7Val	0.297	*var1A1*
MPJ6_CS1015	rs28563878		Exon 1	9481133	34	tgcctttatcctggccactct**T/G**ctgcttccgcggcttggggt	Ser12Ala	0.297	*var1A1*
MPJ6_CS1016	rs12149359		Intron 1	9481099	IVS1+16	ttggggtgagtccttctgaa**A/G**tcaaaatgcggggcacttttt		0.294	*var1A1*

*Number of chromosomes. †Novel variation detected in this study.

Table 4

Frequency of *CES1A2(/1A3)* promoter SNP –816A>C in Japanese cancer patients

CES1A2 and *1A3* Genotype	-816A>C Genotype	Number of subjects	Allele frequency
1A2/1A2	A/A	16	0/32 (0%)
	A/C	0	
	C/C	0	
1A2/1A3	A/A	44	40/166 (24.1%)
	A/C	38	
	C/C	1	
1A3/1A3	A/A	41	48/156 (30.8%)
	A/C	26	
	C/C	11	
Total		177	88/354 (24.9%)

not significant (Table 5). The *CES1* genotypes explained 22.6% of variability in the final model among all the variables and 11.3% of total variability in the AUC ratio.

Effects of CES1 genotypes on SN-38 AUC and toxicity

To clarify the clinical importance of *CES1* genotyping for irinotecan therapy, the effects of *CES1* genotypes or SNPs on AUC levels of the active metabolite SN-38 and neutropenia were examined in the non-*UGT*+/+ patients. In this non-*UGT*+/+ population, significantly higher AUC ratios of (SN-38 + SN-38G)/irinotecan were also observed in the patients with three or four functional *CES1* genes (P = 0.0234, Mann-Whitney test) as observed in all the patients treated with irinotecan monotherapy (Figure 3a). With increased number of functional *CES1* genes, an increasing trend of SN-38 AUC/dose was observed in patients receiving irinotecan monotherapy (1.4-fold for four genes *vs.* two genes; P = 0.080, JT test) (Figure 4). However, multiple regression analysis revealed no statistically significant contribution of *CES1* genotypes to SN-38 AUC/dose although *UGT1A1″*6 or *28″* and *ABCB1*2/*2* showed significant contributions [10]. Regarding neutropenia, a higher incidence (though statistically insignificant) for grade 3/4 neutropenia in patients with four functional *CES1* genes was observed (50% for four genes and 16% for two or three genes, P = 0.09, Fisher's exact test). The effects of the SNPs (–75G>T, –30G>A and –816A>C) on SN-38 AUC or incidence grade 3/4 neutropenia were not significant (data not shown). In platinum-containing regimens, no significant effects of the *CES1* genotypes on SN-38 AUC/dose or incidence of grade 3/4 neutropenia were detected in the non-*UGT*+/+ patients (data not shown).

Discussion

Recent pharmacogenetic studies on irinotecan have shown the clinical significance of *UGT1A1 *6* and *28* in Japanese patients [7,8] and *UGT1A1*28* in Caucasians [5,6] for severe neutropenia. Subsequent studies have revealed additional genetic factors including transporters [10–12]. However, the clinical importance of genotypes of the irinotecan-activating enzymes *CES1* and *CES2* is still uncertain.

Since the hydrolytic activity of CES2 for irinotecan was reported to be much higher than that of CES1 [2], most studies have focused on the clinical significance of *CES2* polymorphisms in irinotecan therapy [13, 14, 22]. We previously identified minor *CES2* genetic variations in Japanese, including *CES2*2* [100C>T (R34W)] and *CES2*5* [1A>T (M1L)] which caused low *in vitro* expression/function of CES2 [13, 14] and also exhibited reduced *in vivo* CES activity in irinotecan-treated patients [14] (also see Figure 3a). However, the major *CES2* haplotypes in Japanese, **1b* (IVS10-108G>A and 1749A>G, frequency = 0.233) and **1c* (–363C>G, IVS10-108G>A and IVS10-87G>A, frequency = 0.027), did not show any significant effects on irinotecan PK [14]. No clinical significance of *CES2* polymorphisms has been reported in Caucasians [22]. Neither *CES1* nor *CES2* SNPs affecting their mRNA expression in normal colonic mucosa were found in European and African populations [23]. Since precise structures of the *CES1* genes and their promoter regions had not been elucidated, evaluation of the roles of the *CES1* genotypes in irinotecan therapy has been rather difficult.

In the present study, the frequencies of individual *CES1* genes (*1A1*, *var1A1*, *1A2* and *1A3*) (Table 2) were almost comparable with the previous report in the Japanese population (0.748, 0.252, 0.313 and 0.687, respectively) [16]. To our knowledge, the present study is the first report suggesting a possible effect of *CES1* genotypes on irinotecan PK. This study showed that the AUC ratio [(SN-38 + SN-38G)/irinotecan], and probably *in vivo* CES activity, was elevated depending on the number of functional *CES1* genes (*1A1*, *var1A1* and *1A2*) in patients treated by irinotecan monotherapy (100 or 150 mg m^{-2} irinotecan) (Figure 3a). This gene-dose effect was not clearly shown in the platinum-containing combination therapy (60–70 mg m^{-2} irinotecan), where renal excretion of irinotecan and its metabolites (especially SN-38G) is highly enhanced by a large volume of infusion fluid. However, the median renal excretion ratio [(SN-38 + SN-38G)/irinotecan] in patients with four functional genes was 1.37-fold higher than that in patients with two or three functional genes in the platinum-containing therapy (data not shown), supporting a partial but significant contribution of the CES1s to activate irinotecan. The present study showed no significant differences in the AUC ratios between *1A1* and *var1A1* (Figure 3a), indicating a common upstream region may be involved in regulation of gene expression of *1A1* and *var1A1*. The previous reports showed the expression levels of CES1A2 were lower than those of CES1A1 [17] and suggested that CES1A2 mRNA was derived mainly from transcription of *var1A1* rather than the original *1A2* [15, 16]. The present study, on the other hand, has suggested that the

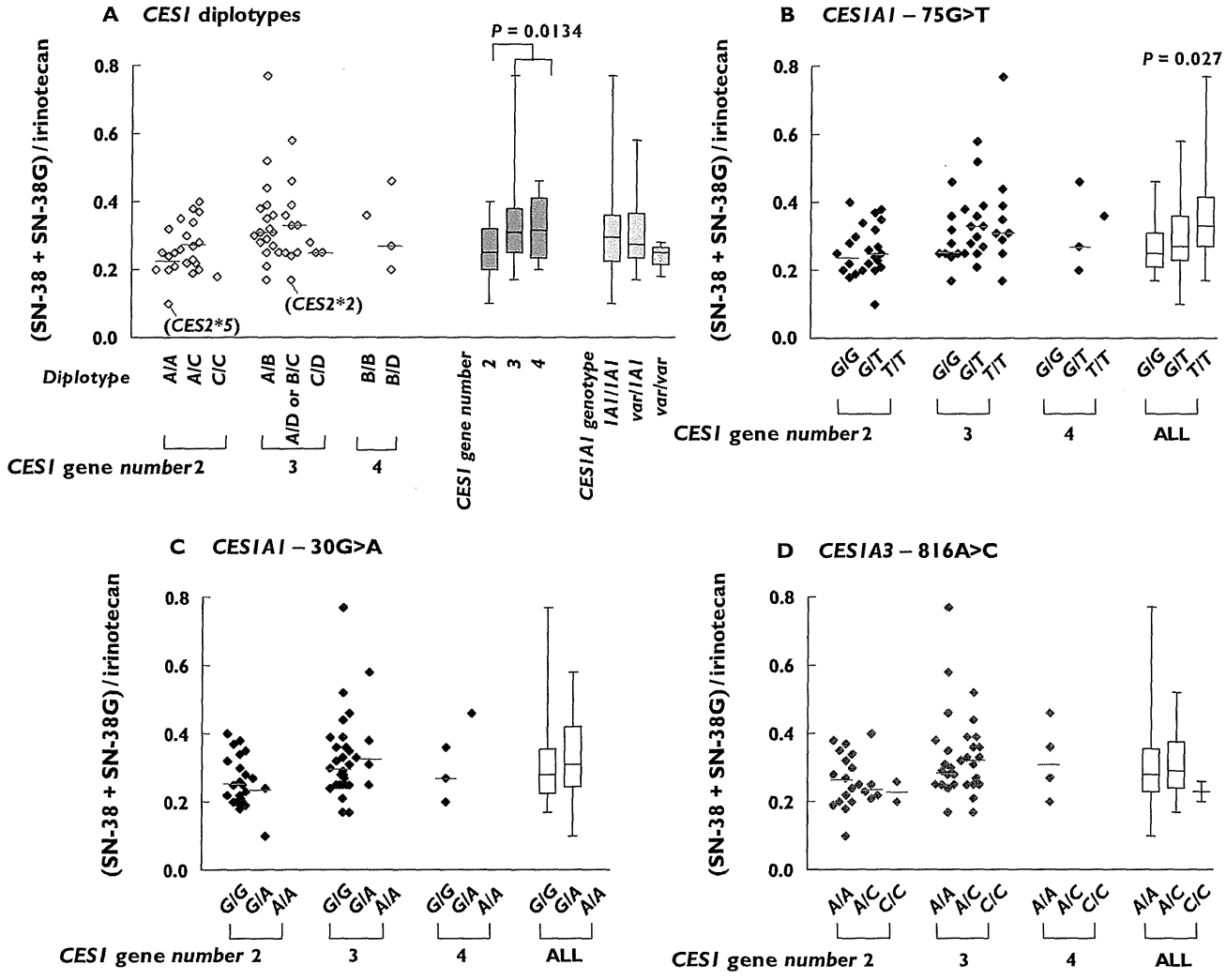

Figure 3

Association of *CES1* diplotypes (A) or SNPs (B–D) with AUC ratio [(SN-38 + SN-38G)/irinotecan], an *in vivo* index of CES activity, in Japanese cancer patients treated with irinotecan monotherapy ($n = 58$). '*CES1* gene number' means the number of functional genes (*1A1*, *var1A1* and *1A2*). Higher AUC ratios were observed in patients with three or four functional *CES1* genes than with two functional genes ($P = 0.0134$, Mann-Whitney test) in (A). Patients with *CES2*5* [*CES2* 1A>T (M1L)] (*CES2*5*) and *CES2*2* [*CES2* 100C>T (R34W)] (*CES2*2*) were found to have reduced CES activity in our previous study [13, 14]

Table 5

Multiple regression analysis of AUC ratio [(SN-38 + SN-38G)/irinotecan]* in Japanese cancer patients treated with irinotecan monotherapy

Variable	Coefficient	SE	*P* value
Smoking	0.073	0.034	0.0375
Initial dose of irinotecan (mg m^{-2})	−0.002	0.001	0.0005
Serum GOT and ALP†	0.082	0.027	0.0038
Serum creatinine (mg dl^{-1})	0.130	0.062	0.0399
***ABCB1*2*‡ (+/+)**	0.042	0.024	0.0831
***CES1* functional gene (n = 3 or 4)**	0.038	0.016	0.0215

$r^2 = 0.500$, Intercept = −0.248, $n = 58$. * Values after logarithmic conversion were used. † Grade 1 or greater for both GOT and ALP. ‡ *ABCB1*2* [2677G>T (A893S)].

1A2 transcript could contribute to the total CES activity because the [(SN-38 + SN-38G)/irinotecan] AUC ratios of patients without *1A2* (with two functional *CES1* genes) were lower than those with *1A2* (with three or four functional genes) (Figure 3a). However, it must be noted that the increase in the AUC ratio by three or four functional *CES1* genes was only 20% compared with two functional genes (Figure 3a), and that such alterations might be masked by other non-genetic factors. In fact, hepatic and renal function, irinotecan dosage and smoking history were found to be potent contributors to this parameter (Table 5).

−816A>C SNP in *1A2* was reported to be associated with imidapril efficacy and a higher promoter activity for

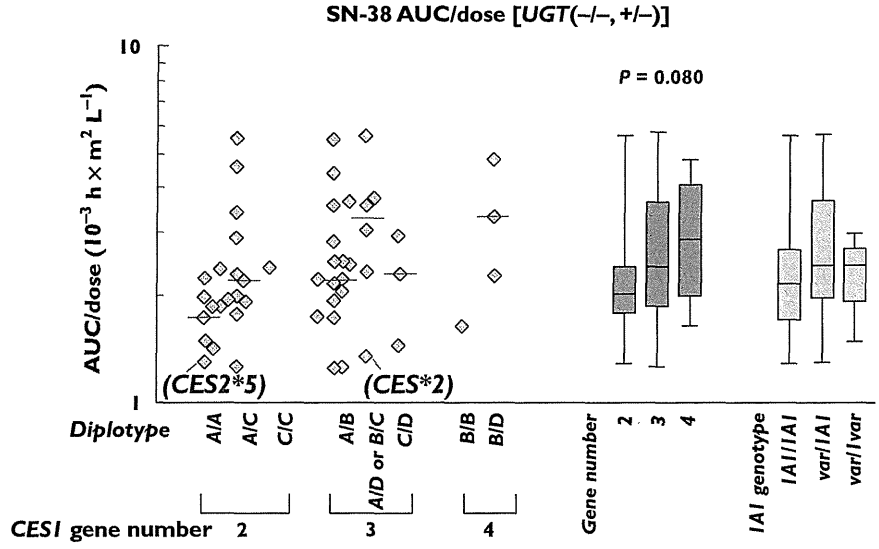

Figure 4

Association of *CES1* genotypes with SN-38 AUC/dose in *UGT*(–/– and +/–) patients treated with irinotecan monotherapy ($n = 51$). '*CES1* gene number' means the number of functional genes (*1A1*, *var1A1* and *1A2*). One patient with an outlying value who had *ABCB1*2* [2677G>T (A893S)] and **14* [2677G>T (A893S) and 1345G>A 230 (E448K)] was excluded from this analysis [10]. A slightly increasing trend in SN-38 AUC(/dose) was observed depending on functional *CES1* gene number. ($P = 0.080$, Jonckheere-Terpstra test). The patients with *CES2*5* [*CES2* 1A>T (M1L)] (*CES2*5*) and *CES2*2* [*CES2* 100C>T (R34W)] (*CES2*2*) [13, 14] are marked

CES1A2 [18] and had strong linkage with SNPs in the proximal promoter region (between –62 to –32) which resulted in additional Sp1 binding sites in the *1A2* promoter region [19]. However, our current study showed no significant effect of –816A>C on the AUC ratio. This can be explained by our finding that –816C and several linked SNPs were mostly located on the *CES1A3* psuedogene but not the functional *1A2* gene.

We newly detected three SNPs (–258C>T, –233C>A and –161A>G) in the 5'-flanking region and one SNP (–30 G>A) in the 5'-UTR of *CES1A1* (Table 3). The effect of –30 G>A on the AUC ratio was not significant (Figure 3c). The frequencies of three other SNPs in the 5'-flanking region were very low (0.003–0.014) which made statistical analysis difficult. These SNPs are not located in the putative transcriptional regulatory regions of *CES1A1*, the binding sites of transcription factors Sp1 and C/EBP [17]. The AUC ratios of the patients with these SNPs were within the 25th–75th percentiles except that slightly higher values were shown in the two -258T patients who received platinum-combination therapy (data not shown). Thus, clinical impact of these SNPs would be small.

With respect to the clinical importance of *CES1* genotyping for irinotecan therapy, the effects of *CES1* genotypes on the AUC level of the active metabolite SN-38 and incidence of grade 3/4 neutropenia should be considered. Since the patients homozygous for *UGT1A1*6 or *28* (*UGT*+/+: **6/*6*, **6/*28* and **28/*28*) showed higher SN-38 AUC/dose levels and severe neutropenia [7], we examined the effects of *CES1* genotypes and SNPs in the non-*UGT*+/+ patients. Increasing trends of SN-38 AUC/dose (Figure 4) and incidence of grade 3/4 neutropenia were observed depending on the functional *CES1* gene number in patients with irinotecan monotherapy although statistical significance was not obtained. For the platinum-containing regimens, no significant effects of *CES1* genotypes were shown. Thus, although possible effects of the *CES1* genotypes on neutropenia could not be excluded in irinotecan monotherapy, this study was still insufficient to establish the clinical importance of *CES1* genotyping in irinotecan therapy. Since the sample size will be twice that of the present study to detect a statistically significant decrease of absolute neutrophil counts in the patients with four functional *CES1* genes, future clinical data obtained in a larger number of patients could clarify this point.

In conclusion, this study suggests that the total number of functional *CES1A* genes could influence the formation of the active metabolite of irinotecan in Japanese cancer patients.

Competing interests

HK has received lecture honorarium from Yakult Honsha, the manufacturer of irinotecan. HM has been paid by Yakult Honsha, the manufacturer of irinotecan, for speaking and research.

This study was supported in part by the Program for the Promotion of Fundamental Studies in Health Sciences of the National Institute of Biomedical Innovation, and by the

Program for the Promotion of Studies in Health Sciences of the Ministry of Health, Labor and Welfare of Japan. We thank Yakult Honsha Co., Ltd. (Tokyo, Japan) for providing analytical standards of irinotecan and its metabolites. We also thank Ms Chie Sudo for her administrative assistance.

REFERENCES

1 Hosokawa M. Structure and catalytic properties of carboxylesterase isozymes involved in metabolic activation of prodrugs. Molecules 2008; 13: 412–31.

2 Humerickhouse R, Lohrbach K, Li L, Bosron WF, Dolan ME. Characterization of CPT-11 hydrolysis by human liver carboxylesterase isoforms hCE-1 and hCE-2. Cancer Res 2000; 60: 1189–92.

3 Ando Y, Saka H, Ando M, Sawa T, Muro K, Ueoka H, Yokoyama A, Saitoh S, Shimokata K, Hasegawa Y. Polymorphisms of UDP-glucuronosyltransferase gene and irinotecan toxicity: a pharmacogenetic analysis. Cancer Res 2000; 60: 6921–6.

4 Iyer L, Das S, Janisch L, Wen M, Ramirez J, Karrison T, Fleming GF, Vokes EE, Schilsky RL, Ratain MJ. UGT1A1*28 polymorphism as a determinant of irinotecan disposition and toxicity. Pharmacogenomics J 2002; 2: 43–7.

5 Innocenti F, Undevia SD, Iyer L, Chen PX, Das S, Kocherginsky M, Karrison T, Janisch L, Ramírez J, Rudin CM, Vokes EE, Ratain MJ. Genetic variants in the UDP-glucuronosyltransferase 1A1 gene predict the risk of severe neutropenia of irinotecan. J Clin Oncol 2004; 22: 1382–8.

6 Han JY, Lim HS, Shin ES, Yoo YK, Park YH, Lee JE, Jang IJ, Lee DH, Lee JS. Comprehensive analysis of UGT1A polymorphisms predictive for pharmacokinetics and treatment outcome in patients with non-small-cell lung cancer treated with irinotecan and cisplatin. J Clin Oncol 2006; 24: 2237–44.

7 Minami H, Sai K, Saeki M, Saito Y, Ozawa S, Suzuki K, Kaniwa N, Sawada J, Hamaguchi T, Yamamoto N, Shirao K, Yamada Y, Ohmatsu H, Kubota K, Yoshida T, Ohtsu A, Saijo N. Irinotecan pharmacokinetics/pharmacodynamics and UGT1A genetic polymorphisms in Japanese: roles of UGT1A1*6 and *28. Pharmacogenet Genomics 2007; 17: 497–504.

8 Sai K, Saito Y, Sakamoto H, Shirao K, Kurose K, Saeki M, Ozawa S, Kaniwa N, Hirohashi S, Saijo N, Sawada J, Yoshida T. Importance of UDP-glucuronosyltransferase 1A1*6 for irinotecan toxicities in Japanese cancer patients. Cancer Lett 2008; 261: 165–71.

9 Sai K, Kaniwa N, Itoda M, Saito Y, Hasegawa R, Komamura K, Ueno K, Kamakura S, Kitakaze M, Shirao K, Minami H, Ohtsu A, Yoshida T, Saijo N, Kitamura Y, Kamatani N, Ozawa S, Sawada J. Haplotype analysis of ABCB1/MDR1 blocks in a Japanese population reveals genotype-dependent renal clearance of irinotecan. Pharmacogenetics 2003; 13: 741–57.

10 Sai K, Saito Y, Maekawa K, Kim SR, Kaniwa N, Nishimaki-Mogami T, Sawada J, Shirao K, Hamaguchi T, Yamamoto N, Kunitoh H, Ohe Y, Yamada Y, Tamura T, Yoshida T, Matsumura Y, Ohtsu A, Saijo N, Minami H. Additive effects of drug transporter genetic polymorphisms on irinotecan pharmacokinetics/pharmacodynamics in Japanese cancer patients. Cancer Chemother Pharmacol 2010; 66: 95–105.

11 Han JY, Lim HS, Park YH, Lee SY, Lee JS. Integrated pharmacogenetic prediction of irinotecan pharmacokinetics and toxicity in patients with advanced non-small cell lung cancer. Lung Cancer 2009; 63: 115–20.

12 Innocenti F, Kroetz DL, Schuetz E, Dolan ME, Ramírez J, Relling M, Chen P, Das S, Rosner GL, Ratain MJ. Comprehensive pharmacogenetic analysis of irinotecan neutropenia and pharmacokinetics. J Clin Oncol 2009; 27: 2604–14.

13 Kubo T, Kim SR, Sai K, Saito Y, Nakajima T, Matsumoto K, Saito H, Shirao K, Yamamoto N, Minami H, Ohtsu A, Yoshida T, Saijo N, Ohno Y, Ozawa S, Sawada J. Functional characterization of three naturally occurring single nucleotide polymorphisms in the CES2 gene encoding carboxylesterase 2 (HCE-2). Drug Metab Dispos 2005; 33: 1482–7.

14 Kim SR, Sai K, Tanaka-Kagawa T, Jinno H, Ozawa S, Kaniwa N, Saito Y, Akasawa A, Matsumoto K, Saito H, Kamatani N, Shirao K, Yamamoto N, Yoshida T, Minami H, Ohtsu A, Saijo N, Sawada J. Haplotypes and a novel defective allele of CES2 found in a Japanese population. Drug Metab Dispos 2007; 35: 1865–72.

15 Tanimoto K, Kaneyasu M, Shimokuni T, Hiyama K, Nishiyama M. Human carboxylesterase 1A2 expressed from carboxylesterase 1A1 and 1A2 genes is a potent predictor of CPT-11 cytotoxicity *in vitro*. Pharmacogenet Genomics 2007; 17: 1–10.

16 Fukami T, Nakajima M, Maruichi T, Takahashi S, Takamiya M, Aoki Y, McLeod HL, Yokoi T. Structure and characterization of human carboxylesterase 1A1, 1A2, and 1A3 genes. Pharmacogenet Genomics 2008; 18: 911–20.

17 Hosokawa M, Furihata T, Yaginuma Y, Yamamoto N, Watanabe N, Tsukada E, Ohhata Y, Kobayashi K, Satoh T, Chiba K. Structural organization and characterization of the regulatory element of the human carboxylesterase (CES1A1 and CES1A2) genes. Drug Metab Pharmacokinet 2008; 23: 73–84.

18 Geshi E, Kimura T, Yoshimura M, Suzuki H, Koba S, Sakai T, Saito T, Koga A, Muramatsu M, Katagiri T. A single nucleotide polymorphism in the carboxylesterase gene is associated with the responsiveness to imidapril medication and the promoter activity. Hypertens Res 2005; 28: 719–25.

19 Yoshimura M, Kimura T, Ishii M, Ishii K, Matsuura T, Geshi E, Hosokawa M, Muramatsu M. Functional polymorphisms in carboxylesterase1A2 (CES1A2) gene involves specific protein 1 (Sp1) binding sites. Biochem Biophys Res Commun 2008; 369: 939–42.

20 Kitamura Y, Moriguchi M, Kaneko H, Morisaki H, Morisaki T, Toyama K, Kamatani N. Determination of probability

distribution of diplotype configuration (diplotype distribution) for each subject from genotypic data using the EM algorithm. Ann Hum Genet 2002; 66: 183–93.

21 Sai K, Saito Y, Fukushima-Uesaka H, Kurose K, Kaniwa N, Kamatani N, Shirao K, Yamamoto N, Hamaguchi T, Kunitoh H, Ohe Y, Tamura T, Yamada Y, Minami H, Ohtsu A, Yoshida T, Saijo N, Sawada J. Impact of CYP3A4 haplotypes on irinotecan pharmacokinetics in Japanese cancer patients. Cancer Chemother Pharmacol 2008; 62: 529–37.

22 Charasson V, Bellott R, Meynard D, Longy M, Gorry P, Robert J. Pharmacogenetics of human carboxylesterase 2, an enzyme involved in the activation of irinotecan into SN-38. Clin Pharmacol Ther 2004; 76: 528–35.

23 Marsh S, Xiao M, Yu J, Ahluwalia R, Minton M, Freimuth RR, Kwok PY, McLeod HL. Pharmacogenomic assessment of carboxylesterases 1 and 2. Genomics 2004; 84: 661–8.

Cancer Science
The official journal of the Japanese Cancer Association

Plasma concentrations of VCAM-1 and PAI-1: A predictive biomarker for post-operative recurrence in colorectal cancer

Yasuhide Yamada,[1,8] Tokuzo Arao,[2,8] Kazuko Matsumoto,[2] Vinita Gupta,[3] Woei Tan,[3] Joe Fedynyshyn,[3] Takako E. Nakajima,[1] Yasuhiro Shimada,[1] Tetsuya Hamaguchi,[1] Ken Kato,[1] Hirokazu Taniguchi,[4] Yutaka Saito,[5] Takahisa Matsuda,[5] Yoshihiro Moriya,[6] Takayuki Akasu,[6] Shin Fujita,[6] Seiichiro Yamamoto[6] and Kazuto Nishio[2,7]

[1]Medical Oncology, National Cancer Center Hospital, Tokyo, Japan; [2]Department of Genome Biology, Kinki University School of Medicine, Osaka, Japan; [3]Bio-Rad Laboratories, Hercules, California, USA; [4]Diagnostic Pathology Division, [5]Endoscopic Division, [6]Surgical Division, National Cancer Center Hospital, Tokyo, Japan

(Received December 2, 2009/Revised March 29, 2010/Accepted April 9, 2010/Accepted manuscript online April 21, 2010/Article first published online May 17, 2010)

This prospective study used antibody suspension bead arrays to identify biomarkers capable of predicting post-operative recurrence with distal metastasis in patients with colorectal cancer. One hundred colorectal cancer patients who underwent surgery were enrolled in this study. The median follow-up period was 3.9 years. The pre-operative plasma concentrations of 24 angiogenesis-related molecules were analyzed with regard to the TNM stage and the development of post-operative recurrence. The concentrations of half of the examined molecules (13/24) increased significantly according to the TNM stage ($P < 0.05$). Meanwhile, a multivariate logistic regression analysis revealed that the concentrations of vascular cell adhesion molecule 1 (VCAM-1) and plasminogen activator inhibitor-1 (PAI-1) were significantly higher in the post-operative recurrence group. The VCAM-1 and PAI-1 model discriminated post-operative recurrence with an area under the curve of 0.82, a sensitivity of 0.75, and a specificity of 0.73. A leave-one-out cross-validation was applied to the model to assess the prediction performance, and the result indicated that the cross-validated error rate was 12.5% (12/96). In conclusion, our results demonstrate that antibody suspension bead arrays are a powerful tool to screen biomarkers in the clinical setting, and the plasma levels of VCAM-1 and PAI-1 together may be a promising biomarker for predicting post-operative recurrence in patients with colorectal cancer. (*Cancer Sci* 2010; 101: 1886–1890)

Colorectal cancer (CRC) is one of the leading causes of death in Japan (http://ganjoho.ncc.go.jp/public/statistics/index.html) and Western countries.[1] Despite recent advances in adjuvant chemotherapy and surgical techniques, 20–40% of patients die because of metastasis after curative surgery.[2] Tumor-node-metastasis (TNM) staging is well established and the most reliable system for predicting the outcome of CRC. In particular, the TNM staging system works very well for predicting the outcome of early stage I cancers and advanced stage IV cancers. However, the 5-year survival rate varies from 44% to 83% within TNM stage III, indicating that a wide variation in outcomes exists within each stage as a result of biological heterogeneity.[3] Thus, highly accurate predictors of post-operative recurrence are needed for patients with CRC who undergo curative surgery, as such predictors would likely contribute to the further improvement of the 5-year survival rate by justifying the addition of intensive adjuvant chemotherapy to the therapeutic regimens of subgroups with a high risk of post-operative recurrence. Therefore, the prediction of post-operative recurrence is regarded as one of the most important research themes in clinical settings and has been extensively studied, with particular attention given to the investigation of various molecular prognostic factors.

In addition to the TNM stage, the carcinoembryonic antigen (CEA) level is routinely used to monitor recurrence in patients with CRC.[4] A large clinical study demonstrated that pre-operative CEA levels provide prognostic information in addition to that provided by the TNM staging system and determined that the pre-operative CEA level was an independent predictor of survival and recurrence.[5] However, the study concluded that although an elevated pre-operative CEA level (>5 mg/mL) may be correlated with a poor prognosis, the available data was insufficient to support the use of the CEA level for determining whether a patient should undergo adjuvant therapy.[4] Other molecular markers, including the K-Ras mutation status,[6,7] microsatellite instability,[8] the loss of heterogeneity at 18q,[9] and p53,[10] have been examined with regard to predicting the outcome of subgroups; unfortunately, none of these molecular markers are suitable for routine clinical use. Thus, further investigations of novel molecular markers are eagerly awaited.

The Bio-Plex suspension array system (Bio-Rad Laboratories, Hercules, CA, USA) utilizes a series of color-coded beads, each of which is coupled to a unique antibody specific for a biochemical marker. This assay is capable of measuring the levels of multiple targets in a single well of a 96-well microplate using as little as 12.5 μL of serum, plasma, or other matrix. In the present study, 24 angiogenesis-related markers from this assay panel were used to evaluate plasma proteins and their potential associations with disease progression and the recurrence of CRC.

Materials and Methods

Patient selection. Patients with histologically confirmed colorectal cancer who were between the ages of 20 and 80 years and who were scheduled to undergo surgery were eligible for enrollment in this study. Additional inclusion criteria included an Eastern Cooperative Oncology Group performance status of 0–2. All the patients in this series underwent surgery. This prospective study was approved by the Institutional Review Board of the National Cancer Center Hospital and written informed consent was obtained from all the patients.

Clinical and pathologic features. Clinical features including age, sex, primary site of tumor, histologic type of tumor, TNM stage, and post-operative recurrence were recorded. A pathologist reviewed the microscopic slides. Post-operative recurrence was defined when distant metastasis was observed. The median follow-up period of post-operative recurrence was 3.9 years.

[7]To whom correspondence should be addressed.
E-mail: knishio@med.kindai.ac.jp
[8]These authors contributed equally to this work.

doi: 10.1111/j.1349-7006.2010.01595.x
© 2010 Japanese Cancer Association

Preparation of plasma samples. Two milliliters of whole blood were collected into EDTA-containing tubes before surgery (within 2 weeks) and were centrifuged at 1500 *g* for 10 min to obtain the plasma samples. The samples were stored at −80°C until further use.

Angiogenesis-related molecules. The 24 plasma markers used in this study were as follows: interleukin 6 receptor (IL-6R), matrix metallopeptidase 9 (MMP-9), TIMP metallopeptidase inhibitor 1 (TIMP-1), TIMP metallopeptidase inhibitor 2 (TIMP-2), endostatin, P-selectin, intercellular adhesion molecule 1 (ICAM-1), vascular cell adhesion molecule 1 (VCAM-1), Tie-2, plasminogen activator inhibitor-1 (PAI-1), macrophage migration inhibitory factor (MIF), plasminogen activator urokinase receptor (uPAR), angiopoietin 2 (Ang-2), follistatin, hepatocyte growth factor (HGF), interleukin 8 (IL-8), colony stimulating factor 3 (G-CSF), platelet-derived growth factor beta polypeptide (PDGF-BB), vascular endothelial growth factor (VEGF), leptin, platelet/endothelial cell adhesion molecule (PECAM-1), interleukin 12 (IL-12), fibroblast growth factor 2 (FGF-basic), and tumor necrosis factor (TNF-α). Ang-2, Follistatin, The nine markers of HGF, IL-8, PDGF-BB, VEGF, Leptin, PECAM-1, and G-CSF are commercially available as the Human Premixed Angiogenesis (9) panel (Bio-Rad Laboratories). The others are available for customization or in developing markers.

Antibody suspension bead arrays system. The plasma concentrations of each molecule were measured using a Bio-Plex suspension array system (Bio-Rad Laboratories), which permits the simultaneous measurement of multiple circulating proteins in a single well using only 12.5 μL of plasma. The assay was performed according to the manufacturer's instructions and a previously described method.[11] All plasma samples were diluted 1 in 4 with the appropriate diluents prior to assay. The samples were tested in duplicate.

Statistical analysis. The correlations between the plasma concentrations and the TNM stages were analyzed using a linear trend analysis and the proportional odds model. In the linear trend analysis, we used a one-way ANOVA model with a linear contrast, which consisted of the TMN stage scores. A *t*-test was used to compare the post-operative recurrence and the no recurrence groups. In the multivariate analysis, an analysis was performed for all the plasma markers but not for the clinical variables because too many explanatory variables for the sample size were included in this study. A logistic regression analysis was used to examine statistical differences according to post-operative recurrence and a stepwise method was used to select the most useful explanatory parameters. Analyses were performed using SAS software version 9.1.3 (SAS Institute, Cary, NC, USA). A *P*-value of <0.05 was considered statistically significant.

Results

Patient results. A total of 100 consecutive patients were enrolled in this study. The median age of the enrolled patients was 59 years (range, 31–79 years). Among them, 96 patients received curative operations and four patients had distal metastasis and received palliative operations. Eleven patients developed recurrences with distal metastasis during the follow-up period. Table 1 summarizes the characteristics of the patients and their tumors.

Plasma concentrations of 24 angiogenesis-related molecules. We measured the plasma concentrations of 24 angiogenesis-related molecules: IL-6R, MMP-9, TIMP-1, TIMP-2, endostatin, P-selectin, ICAM-1, VCAM-1, Tie-2, PAI-1, MIF, uPAR, Ang-2, follistatin, HGF, IL-8, G-CSF, PDGF-BB, VEGF, leptin, PECAM-1, IL-12, FGF-basic, and TNF-α (Table 2). Overall, 98.5% of the plasma samples were successfully quantified using a standard curve.

Table 1. Patient characteristics

Characteristics	Curative ope.		Palliative ope.	Total
	Rec+	Rec−		
Age (years)				
≥60	6	42	2	50
<60	5	43	2	50
Sex				
Male	3	54	3	65
Female	8	31	1	35
Primary site				
Colon	8	40	1	49
Rectum	3	45	3	51
Hist. type				
Well diff.	8	59	3	70
Others	3	26	1	30
TNM stage				
I	1	26	–	27
II	2	22	–	24
III	8	37	–	45
IV	–	–	4	4
Total	11	85	4	100

Hist. type, histology of primary tumor; Rec+, post-operative recurrence (+); Rec−, post-operative recurrence (−).

Tumor-node-metastasis (TNM) stage and plasma concentrations of angiogenesis-related molecules. The TNM stage can be accurately used to stratify patients at a high risk for cancer progression and is thought to reflect the malignant potential of each tumor. To estimate the contributions of the angiogenesis-related molecules to the malignant potentials of the tumors, we examined the correlation between the plasma concentrations of each molecule and the TNM stage. A linear trend analysis showed that the plasma concentrations of 13 molecules increased significantly with an increasing TNM stage ($P < 0.05$): IL-6R, TIMP-1, TIMP-2, P-selectin, Tie-2, PAI-1, uPAR, Ang-2, follistatin, HGF, IL-8, PDGF-BB, and VEGF (Table 3). Next, we performed an exploratory multivariate analysis using a proportional odds model with the TNM stage (I–IV) assigned as the objective variable and each of the angiogenesis-related molecules assigned as explanatory variables. The multivariate analysis identified TIMP-1, P-selectin, Ang-2, HGF, IL-8, PDGF-BB, and VEGF as being significantly correlated with the TNM stage. These results indicated that the plasma concentrations of several molecules increased significantly with an increasing TNM stage, strongly suggesting that these molecules might be candidate biomarkers for an unfavorable outcome in patients with CRC.

Post-operative recurrence and plasma concentrations of angiogenesis-related molecules. To predict post-operative recurrence using this system, we analyzed the 96 patients with CRC who underwent curative operations, excluding the four patients with distal metastasis. Among these 96 patients, 11 developed recurrences during the follow-up period; the remaining 85 patients did not show any signs of recurrence. When the plasma levels of the angiogenesis-related molecules were compared between the patients with recurrences and those without recurrences, *t*-tests demonstrated that the plasma concentrations of IL-6R (63.2 ± 13.8 and 51.3 ± 17.0 ng/mL, respectively), P-selectin (76.1 ± 24.4 and 60.0 ± 24.8 ng/mL, respectively), VCAM-1 (163.9 ± 61.0 and 134.6 ± 35.0 ng/mL, respectively), and PAI-1 (28.2 ± 15.4 and 19.8 ± 10.2 ng/mL, respectively) were significantly higher among the patients with recurrences (Fig. 1a–d, Table 4). A multivariate logistic regression analysis revealed that the plasma concentrations of VCAM-1 and PAI-1 were significantly higher among the patients with recurrences ($P = 0.039$ and $P = 0.028$, respectively). A stepwise

© 2010 Japanese Cancer Association

Table 2. Plasma concentrations of 24 angiogenesis-related molecules in 100 colorectal cancers

Molecules	Range	Average (SD)	25%	Percentile	
	pg/mL			Median	75%
IL-6R	23–149	54 (18)	42	52	62
MMP-9	6–189	35 (27)	20	27	41
TIMP-1	44–283	117 (35)	96	118	135
TIMP-2	9–47	24 (5)	21	24	28
Endostatin	90–456	187 (64)	140	177	223
P-selectin	0–164	64 (27)	48	62	78
ICAM-1	103–605	282 (81)	225	270	317
VCAM-1	76–333	138 (40)	110	135	163
Tie-2	9–1070	143 (164)	48	73	182
PAI-1	3–65	21 (12)	14	19	26
MIF	0–120	53 (26)	44	59	69
uPAR	1–130	24 (23)	8	15	37
Ang-2	0–6147	1381 (1337)	415	938	2197
Follistatin	235–2903	924 (614)	502	686	1197
HGF	201–12213	2700 (2516)	1076	1628	3930
IL-8	5–234	52 (41)	24	34	74
G-CSF	0–4775	832 (1133)	79	247	1161
PDGF-BB	6–6219	737 (831)	220	439	922
VEGF	0–724	186 (164)	67	120	262
Leptin	0–32847	3155 (4433)	1149	2134	3851
PECAM-1	1188–15837	5562 (3472)	2901	4487	7348
IL-12	0–32	5 (6)	2	3	6
FGF-basic	0–235	21 (30)	4	13	25
TNF-α	0–72	4 (9)	1	2	4

The concentrations are ng/mL for interleukin 6 receptor (IL-6R), matrix metallopeptidase 9 (MMP-9), TIMP metallopeptidase inhibitor 1 (TIMP-1), TIMP-2, endostatin, P-selectin, intercellular adhesion molecule 1 (ICAM-1), vascular cell adhesion molecule 1 (VCAM-1), Tie-2, plasminogen activator inhibitor-1 (PAI-1), macrophage migration inhibitory factor (MIF), and plasminogen activator urokinase receptor (uPAR), and the others are pg/mL. FGF-basic, fibroblast growth factor 2; G-CSF, colony stimulating factor 3; HGF, hepatocyte growth factor; PDGF-BB, platelet-derived growth factor beta polypeptide; PECAM-1, platelet/endothelial cell adhesion molecule; TNF-α, tumor necrosis factor; VEGF, vascular endothelial growth factor.

Table 3. Tumor-node-metastasis (TNM) stage and plasma concentrations in 100 colorectal cancers

Molecules	TNM stage				Univariate	Multivariate
	I	II	III	IV	*P*-value	*P*-value
IL-6R	50	57	52	76	0.01	n.s.
MMP-9	34	50	28	33	n.s.	n.s.
TIMP-1	107	122	114	185	<0.0001	0.02
TIMP-2	24	24	24	33	0.003	n.s.
Endostatin	184	198	182	201	n.s.	n.s.
P-selectin	56	67	63	109	0.0003	0.04
ICAM-1	276	315	266	298	n.s.	n.s.
VCAM-1	135	136	141	144	n.s.	n.s.
Tie-2	116	162	129	375	0.005	n.s.
PAI-1	18	24	21	38	0.003	n.s.
MIF	53	55	51	78	n.s.	n.s.
uPAR	20	27	22	53	0.01	n.s.
Ang-2	978	1458	1447	2914	0.007	0.03
Follistatin	778	953	928	1704	0.006	n.s.
HGF	1933	2932	2803	5342	0.01	0.04
IL-8	38	56	53	108	0.002	0.02
G-CSF	595	1114	797	1132	n.s.	n.s.
PDGF-BB	442	822	802	1483	0.02	0.03
VEGF	129	209	192	375	0.006	0.03
Leptin	3236	2815	3235	3752	n.s.	n.s.
PECAM-1	5026	5914	5625	6356	n.s.	n.s.
IL-12	3	8	5	5	n.s.	n.s.
FGF-basic	19	32	16	28	n.s.	n.s.
TNF-α	4	6	3	2	n.s.	n.s.

Values indicate the average. Univariate: linear trend analysis, multivariate: proportional odds model. The concentrations are ng/mL for interleukin 6 receptor (IL-6R), matrix metallopeptidase 9 (MMP-9), TIMP metallopeptidase inhibitor 1 (TIMP-1), TIMP-2, endostatin, P-selectin, intercellular adhesion molecule 1 (ICAM-1), vascular cell adhesion molecule 1 (VCAM-1), Tie-2, plasminogen activator inhibitor-1 (PAI-1), macrophage migration inhibitory factor (MIF), and plasminogen activator urokinase receptor (uPAR), and the others are pg/mL. FGF-basic, fibroblast growth factor 2; G-CSF, colony stimulating factor 3; HGF, hepatocyte growth factor; n.s., not significant; PDGF-BB, platelet-derived growth factor beta polypeptide; PECAM-1, platelet/endothelial cell adhesion molecule; TNF-α, tumor necrosis factor; VEGF, vascular endothelial growth factor.

method selected VCAM-1 and PAI-1 as the most useful explanatory parameters, suggesting that the combination of these two molecules might synergistically improve the prediction of post-operative recurrence. Finally, a prediction model incorporating VCAM-1 and PAI-1 successfully discriminated post-operative recurrence, with an area under the curve (AUC) of 0.82, a sensitivity of 0.75, and a specificity of 0.73 (Fig. 2a). To assess the prediction performance, a leave-one-out cross-validation was applied to the model. The cross-validated error rate was 12.5% (12/96). In stage III patients, the prediction model had a sensitivity of 0.625 (5/8) and a specificity of 0.865 (32/37) for predicting post-operative recurrence (Fig. S2). On the other hand, when apparent distal metastases of CRCs were applied to the VCAM-1/PAI-1 prediction model, three out of four metastatic cases were determined as "recurrence (+) cases". These results suggest that apparent metastatic tumors could be discriminated using the model. Although a validation study is necessary, our results raise the possibility that the combined use of the pre-operative plasma concentrations of VCAM-1 and PAI-1 might be useful for predicting post-operative recurrence in patients with CRC. Finally, we retrospectively analyzed the plasma PAI-1 concentrations of metastatic and non-metastatic CRC in another study of an independent cohort using conventional ELISA. The plasma concentrations in the metastatic CRC patients were significantly higher than those in the non-metastatic patients ($P = 0.005$), even in the independent cohort (Fig. S1). The CEA level was not significantly different between the recurrence (+) *versus* the recurrence (−) groups ($P = 0.335$) in our study.

Discussion

Vascular cell adhesion molecule 1 (VCAM-1)/CD106 is a member of the Ig superfamily and encodes a cell surface sialoglycoprotein expressed by cytokine-activated endothelium. This type I membrane protein mediates leukocyte-endothelial cell adhesion and signal transduction, and may play a role in the development of atherosclerosis[12] and rheumatoid arthritis.[13] In the field of oncology, accumulating evidence suggests that VCAM-1 is associated with a poor outcome.[14–17] Recently, Shariat *et al.*[18] reported that standard clinical variables alone exhibited an accuracy of 71.6% for predicting the risk of biochemical recurrence following a radical prostatectomy in patients with prostate cancer, whereas the addition of preoperative blood levels of TGF-β1, sIL-6R, IL-6, VCAM-1, VEGF, endoglin, and uPA increased the predictive accuracy by 15–86.6%. Vascular endothelial growth factor (VEGF) and uPA were not significant predictors of post-operative recurrence in our data set for CRC, but VCAM-1 and sIL-6R were significant, consistent with Shariat's study. The mechanism by which VCAM-1 mediates an unfavorable phenotype remains unclear, but the most probable explanation is that the tumor cells escape T-cell immunity by

doi: 10.1111/j.1349-7006.2010.01595.x
© 2010 Japanese Cancer Association

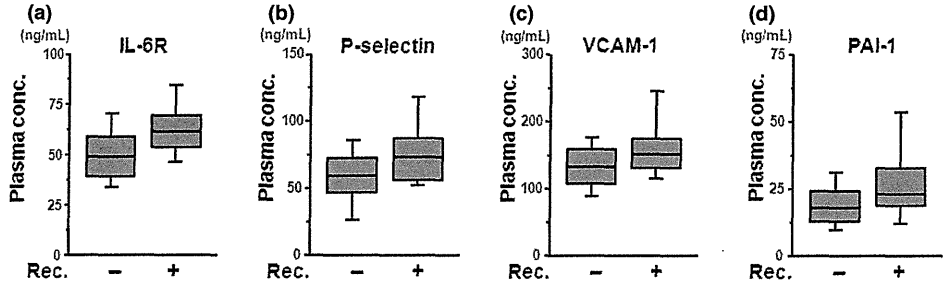

Fig. 1. The concentrations of (a) interleukin 6 receptor (IL-6R), (b) P-selectin, (c) vascular cell adhesion molecule 1 (VCAM-1), and (d) plasminogen activator inhibitor-1 (PAI-1) were significantly higher in the recurrence group in colorectal cancer. The upper bar, box, and lower bar represent the 90%, 75%, 50%, 25% and 10% percentiles. The plasma concentrations of each molecule were measured using a Bio-Plex suspension array system. Rec, recurrence.

Table 4. Results of multivariate analysis for recurrence after curative surgery in 96 colorectal cancers

Molecules	Recurrence*		Univariate		Multivariate
	+	–	*t*-test	Logistic	Stepwise
			P-value	*P*-value	*P*-value
IL-6R	63	51	0.03	n.s.	
MMP-9	37	35	n.s.	n.s.	
TIMP-1	119	113	n.s.	n.s.	
TIMP-2	25	24	n.s.	n.s.	
Endostatin	193	186	n.s.	n.s.	
P-selectin	76	60	0.04	n.s.	
ICAM-1	285	281	n.s.	n.s.	
VCAM-1	164	135	0.02	0.039	0.009
Tie-2	183	127	n.s.	n.s.	
PAI-1	28.3	19.8	0.02	0.005	0.005
MIF	64	51	n.s.	n.s.	
uPAR	30	21	n.s.	n.s.	
Ang-2	1514	1292	n.s.	n.s.	
Follistatin	962	883	n.s.	n.s.	
HGF	3155	2517	n.s.	n.s.	
IL-8	53	49	n.s.	n.s.	
G-CSF	892	810	n.s.	n.s.	
PDGF-BB	972	671	n.s.	n.s.	
VEGF	211	174	n.s.	n.s.	
Leptin	2623	3196	n.s.	n.s.	
PECAM-1	6159	5447	n.s.	n.s.	
IL-12	4	5	n.s.	n.s.	
FGF-basic	16	22	n.s.	n.s.	
TNF-α	4	4	n.s.	n.s.	

*Values indicate the average. Recurrence, post-operative recurrence; logistic, logistic regression model. The concentrations are ng/mL for interleukin 6 receptor (IL-6R), matrix metallopeptidase 9 (MMP-9), TIMP metallopeptidase inhibitor 1 (TIMP-1), TIMP-2, endostatin, P-selectin, intercellular adhesion molecule 1 (ICAM-1), vascular cell adhesion molecule 1 (VCAM-1), Tie-2, plasminogen activator inhibitor-1 (PAI-1), macrophage migration inhibitory factor (MIF), and plasminogen activator urokinase receptor (uPAR), and the others are pg/mL. FGF-basic, fibroblast growth factor 2; G-CSF, colony stimulating factor 3; HGF, hepatocyte growth factor; n.s., not significant; PDGF-BB, platelet-derived growth factor beta polypeptide; PECAM-1, platelet/endothelial cell adhesion molecule; TNF-α, tumor necrosis factor; VEGF, vascular endothelial growth factor.

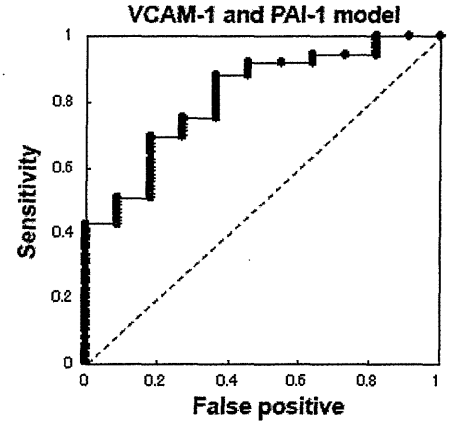

Fig. 2. The receiver–operator curve (ROC) for post-operative recurrence. A stepwise method selected vascular cell adhesion molecule 1 (VCAM-1) and plasminogen activator inhibitor-1 (PAI-1) as the most useful explanatory parameters; these two molecules were subsequently used to construct a prediction model. The ROC indicates the results of this model, which was capable of discriminating post-operative recurrence with an area under the curve (AUC) of 0.82, a sensitivity of 0.75, and a specificity of 0.73.

overexpressing the endothelial cell adhesion molecule VCAM-1, which normally mediates leukocyte extravasation to sites of tissue inflammation.[19]

Plasminogen activator inhibitor-1 (PAI-1)/SERPINE1 belongs to the plasmin/plasminogen system and is secreted into the blood, where it prevents the generation of plasmin, promoting the persistence and expansion of thrombi.[20] Plasminogen activator inhibitor-1 (PAI-1) is known as tumor biological prognostic factor and has been thoroughly validated with regard to its clinical utility in breast cancer.[21,22] The 2007 Breast Tumor Markers Guidelines recommend that uPA/PAI-1 be measured using an ELISA with a minimum of 300 mg of fresh or frozen breast cancer tissue for determining the prognosis of patients with newly diagnosed, node-negative breast cancer. Furthermore, CMF-based adjuvant chemotherapy provides a substantial benefit, compared with observation alone, in patients with a high risk of recurrence as determined by the presence of high levels of uPA and PAI-1.[23] Previous reports have demonstrated that higher levels of PAI-1, but not PAI-2, are associated with large tumors, metastatic stage, and a worse prognosis in patients with CRC.[24–26] Our study differed in that it evaluated the clinical parameter of post-operative recurrence in a prospective study. The biological mechanism by which PAI-1 promotes tumor progression is thought to involve a reduction in cell adhesion to the extracellular matrix as a consequence of excess PAI-1 interfering with uPAR binding to vitronectin, thereby facilitating cell invasion and migration.[27] Interestingly, accumulating data indicate that both VCAM-1 and PAI-1 promote tumor metastasis and cellular adhesion. These activities are likely involved in post-operative recurrence. We plan to perform

© 2010 Japanese Cancer Association

a validation study to predict post-operative recurrence using the plasma concentrations of VCAM-1 and PAI-1 in the near future.

In conclusion, we have demonstrated that a combination prediction model based on the plasma concentrations of VCAM-1 and PAI-1 was a useful biomarker for predicting post-operative recurrence in patients with colorectal cancer. Our strategy, which utilizes a multiplex immunoassay system, may be a powerful tool for identifying biomarkers in clinical settings.

Acknowledgments

This study was supported by the Third-Term Comprehensive 10-Year Strategy for Cancer Control, a Grant-in-Aid for Scientific Research; the Program for the Promotion of Fundamental Studies in Health Sciences of the National Institute of Biomedical Innovation (NiBio); a Grant-in-Aid for Cancer Research (H20-20-9) from the Ministry of Health, Labour and Welfare; and a Grant-in-Aid for Scientific Research from the Ministry of Education, Culture, Sports, Science and Technology of Japan (19209018). The following people have played very important roles in the conduct of this project: Hiromi Orita, Hideko Morita, and Mari Araake.

Disclosure Statement

The authors have no conflict of interest.

References

1 Greenlee RT, Hill-Harmon MB, Murray T, Thun M. Cancer statistics, 2001. *CA Cancer J Clin* 2001; **51**: 15–36.
2 Ratto C, Sofo L, Ippoliti M, Merico M, Doglietto GB, Crucitti F. Prognostic factors in colorectal cancer. Literature review for clinical application. *Dis Colon Rectum* 1998; **41**: 1033–49.
3 Mutch MG. Molecular profiling and risk stratification of adenocarcinoma of the colon. *J Surg Oncol* 2007; **96**: 693–703.
4 Locker GY, Hamilton S, Harris J *et al.*; ASCO. ASCO 2006 update of recommendations for the use of tumor markers in gastrointestinal cancer. *J Clin Oncol* 2006;**24**:5313–27.
5 Park YJ, Park KJ, Park JG, Lee KU, Choe KJ, Kim JP. Prognostic factors in 2230 Korean colorectal cancer patients: analysis of consecutively operated cases. *World J Surg* 1999; **23**: 721–6.
6 Andreyev HJ, Norman AR, Cunningham D, Oates JR, Clarke PA. Kirsten ras mutations in patients with colorectal cancer: the multicenter "RASCAL" study. *J Natl Cancer Inst* 1998; **90**: 675–84.
7 Andreyev HJ, Norman AR, Cunningham D *et al.* Kirsten ras mutations in patients with colorectal cancer: the 'RASCAL II' study. *Br J Cancer* 2001; **85**: 692–6.
8 Popat S, Hubner R, Houlston RS. Systematic review of microsatellite instability and colorectal cancer prognosis. *J Clin Oncol* 2005; **23**: 609–18.
9 Aschele C, Debernardis D, Lonardi S *et al.* Deleted in colon cancer protein expression in colorectal cancer metastases: a major predictor of survival in patients with unresectable metastatic disease receiving palliative fluorouracil-based chemotherapy. *J Clin Oncol* 2004; **22**: 3758–65.
10 Duffy MJ, van Dalen A, Haglund C *et al.* Tumour markers in colorectal cancer: European Group on Tumour Markers (EGTM) guidelines for clinical use. *Eur J Cancer* 2007; **43**: 1348–60.
11 Kimura H, Kasahara K, Sekijima M, Tamura T, Nishio K. Plasma MIP-1beta levels and skin toxicity in Japanese non-small cell lung cancer patients treated with the EGFR-targeted tyrosine kinase inhibitor, gefitinib. *Lung Cancer* 2005; **50**: 393–9.
12 Galkina E, Ley K. Vascular adhesion molecules in atherosclerosis. *Arterioscler Thromb Vasc Biol* 2007; **27**: 2292–301.
13 Carter RA, Wicks IP. Vascular cell adhesion molecule 1 (CD106): a multifaceted regulator of joint inflammation. *Arthritis Rheum* 2001; **44**: 985–94.
14 Yao M, Huang Y, Shioi K *et al.* A three-gene expression signature model to predict clinical outcome of clear cell renal carcinoma. *Int J Cancer* 2008; **123**: 1126–32.
15 De Cicco C, Ravasi L, Zorzino L *et al.* Circulating levels of VCAM and MMP-2 may help identify patients with more aggressive prostate cancer. *Curr Cancer Drug Targets* 2008; **8**: 199–206.
16 Silva HC, Garcao F, Coutinho EC, De Oliveira CF, Regateiro FJ. Soluble VCAM-1 and E-selectin in breast cancer: relationship with staging and with the detection of circulating cancer cells. *Neoplasma* 2006; **53**: 538–43.
17 Shioi K, Komiya A, Hattori K *et al.* Vascular cell adhesion molecule 1 predicts cancer-free survival in clear cell renal carcinoma patients. *Clin Cancer Res* 2006; **12**: 7339–46.
18 Shariat SF, Karam JA, Walz J *et al.* Improved prediction of disease relapse after radical prostatectomy through a panel of preoperative blood-based biomarkers. *Clin Cancer Res* 2008; **14**: 3785–91.
19 Wu TC. The role of vascular cell adhesion molecule-1 in tumor immune evasion. *Cancer Res* 2007; **67**: 6003–6.
20 Durand MK, Bødker JS, Christensen A *et al.* Plasminogen activator inhibitor-I and tumour growth, invasion, and metastasis. *Thromb Haemost* 2004; **91**: 438–49.
21 Harbeck N, Schmitt M, Kates RE *et al.* Clinical utility of urokinase-type plasminogen activator and plasminogen activator inhibitor-1 determination in primary breast cancer tissue for individualized therapy concepts. *Clin Breast Cancer* 2002; **3**: 196–200.
22 Harbeck N, Kates RE, Schmitt M. Clinical relevance of invasion factors urokinase-type plasminogen activator and plasminogen activator inhibitor type 1 for individualized therapy decisions in primary breast cancer is greatest when used in combination. *J Clin Oncol* 2002; **20**: 1000–7.
23 Harris L, Fritsche H, Mennel R *et al.* American Society of Clinical Oncology. American Society of Clinical Oncology 2007 update of recommendations for the use of tumor markers in breast cancer. *J Clin Oncol* 2007; **25**: 5287–312.
24 Herszènyi L, Plebani M, Carraro P *et al.* The role of cysteine and serine proteases in colorectal carcinoma. *Cancer* 1999; **86**: 1135–42.
25 Sier CF, Vloedgraven HJ, Ganesh S *et al.* Inactive urokinase and increased levels of its inhibitor type 1 in colorectal cancer liver metastasis. *Gastroenterology* 1994; **107**: 1449–56.
26 Langenskiöld M, Holmdahl L, Angenete E, Falk P, Nordgren S, Ivarsson ML. Differential prognostic impact of uPA and PAI-1 in colon and rectal cancer. *Tumour Biol* 2009; **30**(4): 210–20.
27 Berger DH. Plasmin/plasminogen system in colorectal cancer. *World J Surg* 2002; **26**: 767–71.

Supporting Information

Additional Supporting Information may be found in the online version of this article:

Fig. S1. Metastasis (+) *vs* (−) in independent samples of colorectal cancer (CRC) (n = 28).

Fig. S2. Post-operative recurrence (+) *vs* (−) in stage III colorectal cancer (CRC) (n = 45).

Please note: Wiley-Blackwell are not responsible for the content or functionality of any supporting materials supplied by the authors. Any queries (other than missing material) should be directed to the corresponding author for the article.

doi: 10.1111/j.1349-7006.2010.01595.x
© 2010 Japanese Cancer Association

Published OnlineFirst February 9, 2010; DOI: 10.1158/0008-5472.CAN-09-2161

Tumor and Stem Cell Biology

Cancer Research

FOXQ1 Is Overexpressed in Colorectal Cancer and Enhances Tumorigenicity and Tumor Growth

Hiroyasu Kaneda[1,2], Tokuzo Arao[1], Kaoru Tanaka[1,2], Daisuke Tamura[1], Keiichi Aomatsu[1], Kanae Kudo[1], Kazuko Sakai[1], Marco A. De Velasco[1], Kazuko Matsumoto[1], Yoshihiko Fujita[1], Yasuhide Yamada[3], Junji Tsurutani[2], Isamu Okamoto[2], Kazuhiko Nakagawa[2], and Kazuto Nishio[1]

Abstract

Forkhead box Q1 (FOXQ1) is a member of the forkhead transcription factor family, and it has recently been proposed to participate in gastric acid secretion and mucin gene expression in mice. However, the role of FOXQ1 in humans and especially in cancer cells remains unknown. We found that *FOXQ1* mRNA is overexpressed in clinical specimens of colorectal cancer (CRC; 28-fold/colonic mucosa). A microarray analysis revealed that the knockdown of *FOXQ1* using small interfering RNA resulted in a decrease in $p21^{CIP1/WAF1}$ expression, and a reporter assay and a chromatin immunoprecipitation assay showed that *p21* was one of the target genes of FOXQ1. Stable FOXQ1-overexpressing cells (H1299/FOXQ1) exhibited elevated levels of p21 expression and inhibition of apoptosis induced by doxorubicin or camptothecin. Although cellular proliferation was decreased in H1299/FOXQ1 cells *in vitro*, H1299/FOXQ1 cells significantly increased tumorigenicity [enhanced green fluorescent protein (EGFP): 2/15, FOXQ1: 7/15] and enhanced tumor growth (437 ± 301 versus 1735 ± 769 mm^3, $P < 0.001$) *in vivo*. Meanwhile, stable p21 knockdown of H1299/FOXQ1 cells increased tumor growth, suggesting that FOXQ1 promotes tumor growth independent of p21. Microarray analysis of H1299/EGFP and H1299/FOXQ1 revealed that FOXQ1 overexpression upregulated several genes that have positive roles for tumor growth, including *VEGFA, WNT3A, RSPO2,* and *BCL11A*. CD31 and terminal deoxynucleotidyl transferase-mediated dUTP nick end labeling staining of the tumor specimens showed that FOXQ1 overexpression mediated the angiogenic and antiapoptotic effect *in vivo*. In conclusion, FOXQ1 is overexpressed in CRC and enhances tumorigenicity and tumor growth presumably through its angiogenic and antiapoptotic effects. Our findings show that FOXQ1 is a new member of the cancer-related FOX family. *Cancer Res; 70(5); 2053–63. ©2010 AACR.*

Introduction

The forkhead box (*Fox*) gene family is a large and diverse group of transcription factors that share certain characteristics of a conserved, ~100 amino acid DNA-binding motif known as the forkhead or winged helix domain; over 100 proteins with forkhead domains have been identified, comprising at least 17 subclasses to date (1). The Fox gene family plays various important roles, not only in biological processes including development, metabolism, immunology, and senescence but also in cancer development (2, 3).

Authors' Affiliations: Departments of [1]Genome Biology and [2]Medical Oncology, Kinki University School of Medicine, Osaka-Sayama, Osaka, Japan and [3]Department of Medical Oncology, National Cancer Center Hospital, Chuo-ku, Tokyo, Japan

Note: Supplementary data for this article are available at Cancer Research Online (http://cancerres.aacrjournals.org/).

Corresponding Author: Kazuto Nishio, Department of Genome Biology, Kinki University School of Medicine, 377-2 Ohno-higashi, Osaka-Sayama, Osaka 589-8511, Japan. Phone: 81-72-366-0221; Fax: 81-72-366-0206; E-mail: knishio@med.kindai.ac.jp.

doi: 10.1158/0008-5472.CAN-09-2161

©2010 American Association for Cancer Research.

Forkhead box Q1 (*FOXQ1*, also known as HFH1) is a member of the FOX gene family and contains the core DNA binding domain, whereas the flanking wings of FOXQ1 contribute to its sequence specificity (4). As a transcription factor, FOXQ1 is known to repress the promoter activity of smooth muscle–specific genes, such as telokin and SM22α, in A10 vascular muscle cells (5), and FOXQ1 expression is regulated by Hoxa1 in embryonic stem cells (6). The biological function of *Foxq1* has been clearly identified in hair follicle differentiation in satin (sa) homozygous mice (7); interestingly, satin mice also exhibit suppressed natural killer cell function and T-cell function, suggesting a relation with immunology. Satin mice have provided evidence that Hoxc13 regulates foxq1 expression and that "cross-talk" occurs between Homeobox and Fox (8). Foxq1 mRNA is widely expressed in murine tissues, with particularly high expression levels in the stomach and bladder (5). Recently, two important findings have been reported regarding its involvement in stomach surface cells. Foxq1-deficient mice exhibit a lack of gastric acid secretion in response to various secretagogue stimuli (9). On the other hand, Foxq1 regulates gastric MUC5AC synthesis, providing clues as to the lineage-specific cell differentiation in gastric surface epithelia (10). Despite accumulating evidence supporting the biological function of the murine foxq1 gene in hair follicle

Downloaded from cancerres.aacrjournals.org on March 20, 2013. © 2010 American Association for Cancer Research.

Published OnlineFirst February 9, 2010; DOI: 10.1158/0008-5472.CAN-09-2161

morphogenesis and gastric epithelial cells, no data regarding the cellular and biological functions of human *FOXQ1*, especially in cancer cells, are available.

$p21^{CIP1/WAF1}$ (hereafter called p21) is a member of the cip/kip family of cyclin kinase inhibitors, and initial reports have shown that p21 functions as a G_1 cyclin kinase inhibitor (11, 12) and a downstream molecule of p53 (13). p21 possesses a variety of cellular functions, including the negative modulation of cell cycle progression (14), cellular differentiation (15), and the regulation of p53-dependent antiapoptosis (reviewed in ref. 16). The expression of p21 is regulated by both p53-dependent and p53-independent mechanisms at the transcriptional level. Other regulatory mechanisms of p21 expression involve proteasome-mediated degradation, mRNA stability, alterations in the epigenetic silencing of the p21 promoter, and secondary decreases resulting from viral activity targeting p53, such as the activities of human papilloma virus and hepatitis C virus (17). However, its expression is considered to be regulated mainly at the transcriptional level (18). Accumulating data indicate that many molecules from diverse signaling pathways can activate or repress the p21 promoter, including p53, transforming growth factor-β (TGF-β), c-jun, Myc, Sp1/Sp3, signal transducers and activators of transcriptions, CAAT/enhancer binding protein-α (C/EBP-α), C/EBP-β, basic helix-loop-helix proteins, and myogenic differentiation 1 (reviewed in ref. 19). Thus, p21 is integrally involved in both cell cycle and apoptosis; therefore, identifying its regulatory molecules is of great importance.

We performed a microarray analysis of clinical samples of paired colorectal cancer (CRC) specimens and normal colonic mucosa specimens to identify genes that were overexpressed in CRC. Our results revealed that *FOXQ1* gene expression was ~28-fold higher in CRC than in normal colonic mucosa, and we hypothesized that FOXQ1 may play a role in CRC. In the present study, we investigated the biological function of FOXQ1.

Materials and Methods

Antibodies. The following antibodies were used: anti-p21, anti-p53, anti-cdk2, anti-cdk4, anti-cyclin D, anti-phosphorylated Rb, anti-poly(ADP-ribose) polymerase (PARP), anti-cleaved PARP, anti-caspase-3, anti-cleaved caspase-3, secondary antibodies, and Myc-tag mouse antibody (Cell Signaling), as well as anti-β-actin (Santa Cruz Biotechnology). A mouse anti-CD31 monoclonal antibody was purchased from BD Biosciences.

Cell lines and cultures. The DLD-1, MKN74, H1299, SBC3, and U251 cell lines were cultured in RPMI 1640 (Sigma). The WiDr, CoLo320DM, and human embryonic kidney cell line 293 (HEK293) cell lines were cultured in DMEM (Sigma), and the LoVo cell line was cultured in Ham/F12 medium [Life Technologies Bethesda Research Laboratories (BRL)]. All media were supplemented with 10% heat-inactivated fetal bovine serum (Life Technologies BRL), and the cell lines were maintained in a 5% CO_2-humidified atmosphere at 37°C.

Patients and samples. Paired CRC and noncancerous colonic mucosa samples were evaluated using a microarray analysis in the first consecutive 10 patients. These samples and another 36 CRC samples were analyzed using real-time reverse transcription–PCR (RT-PCR). The RNA extraction method and the quality check protocol have been previously described (20). This study was approved by the institutional review board of the National Cancer Center Hospital, and written informed consent was obtained from all the patients.

Plasmid construction, viral production, and stable transfectants. The cDNA fragment encoding human full-length FOXQ1 was isolated using PCR and Prime STAR HS DNA polymerase (TaKaRa) with 5′-GGG AAT TCG CGG CCA TGA AGT TGG AGG TCT TCG TC-3′ and 5′-CCC TCG AGC GCT ACT CAG GCT AGG AGC GTC TCC AC-3′ sense and antisense primers, respectively. The methods used in this section have been previously described (21). Short hairpin RNA (shRNA) targeting p21 was constructed using oligonucleotides encoding small interfering RNA (siRNA) directed against p21 and a nonspecific target as follows: 5′-CTA AGA GTG CTG GGC ATT TTT-3′ for p21 shRNA and 5′-TGT TCG CAG TAC GGT AAT GTT-3′ for control shRNA. They were cloned into an RNAi-Ready pSIREN-RetroQZsGreen vector (Clontech) according to manufacturer's protocol. The stable transfectants expressing enhanced green fluorescent protein (EGFP) or FOXQ1 or FOXQ1 with shRNA targeting p21 for each cell line were designated as HEK293/EGFP, HEK293/FOXQ1, CoLo320/EGFP, CoLo320/FOXQ1, H1299/EGFP, H1299/FOXQ1, H1299/FOXQ1/sh-control, and H1299/FOXQ1/sh-p21. The FOXQ1 human cDNA was tagged at the NH_2 terminus with the myc epitope using the pCMV-Myc vector (Clontech) for chromatin immunoprecipitation (ChIP) assay.

SiRNA transfection. Two different sequences of siRNA targeting human FOXQ1 and negative control siRNA were purchased from QIAGEN. The sequences of FOXQ1 and control siRNA were as follows: FOXQ1#1 sense, 5′-CCA UCA AAC GUG CCU UAA A-3′ and antisense, 5′-UUU AAG GCA CGU UUG AUG G-3′; FOXQ1#4 sense, 5′-CGC GGA CUU UGC ACU UUG A-3′ and antisense, 5′-UCA AAG UGC AAA GUC CGC G-3′; control siRNA (scramble) sense, 5′-UUC UCC GAA CGU GUC ACG U-3′ and antisense, 5′-ACG UGA CAC GUU CGG AGA A-3′; control siRNA (GFP) sense, 5′-GCA AGC UGA CCC UGA AGU UCA U-3′ and antisense, 5′-GAA CUU CAG GGU CAG CUU GCC G-3′. The methods of transfection have been previously described (22).

Real-time RT-PCR and Western blot analysis. The methods used in this section have been previously described (21). The primers used for real-time RT-PCR were purchased from Takara as follows: FOXQ1 forward, 5′-CGC GGA CTT TGC ACT TTG AA-3′ and reverse, 5′-AGC TTT AAG GCA CGT TTG ATG GAG-3′; p21 forward, 5′-TCC AGC GAC CTT CCT CAT CCA C-3′ and reverse, 5′-TCC ATA GCC TCT ACT GCC ACC ATC-3′; glyceraldehyde-3-phosphate dehydrogenase (GAPD) forward, 5′-GCA CCG TCA AGG CTG AGA AC-3′ and reverse, 5′-ATG GTG GTG AAG ACG CCA GT-3′. The experiment was performed in triplicate.

Downloaded from cancerres.aacrjournals.org on March 20, 2013. © 2010 American Association for Cancer Research.

Published OnlineFirst February 9, 2010; DOI: 10.1158/0008-5472.CAN-09-2161

Luciferase reporter assay. The human p21 promoter reporter vector was constructed according to a previously described method (13). The p21 promoter fragment was cut between the *Kpn*I and *Xho*I restriction sites and was transferred into the luciferase reporter vector pGL4.14 (Promega). All sequences were verified using DNA sequencing. The empty and p21 promoter-containing reporter vectors were designated as pGL4.14-mock and pGL4.14-p21, respectively. All the samples were examined in triplicate.

ChIP. ChIP was carried out using the ChIP-IT Express Enzymatic kit (Active Motif) according to manufacturer's protocol. HEK293 cells were transfected with empty vector (Myc) or Myc-tagged FOXQ1 vector. The putative region of the p21 promoter (−2264 to −1971) was amplified with the following primers: 5′-TTG AGC TCT GGC ATA GAA GA-3′ (forward) and 5′-TAC CCA GAC ACA CTC TAA GG-3′ (reverse). As a negative control, the glyceraldehyde-3-phosphate dehydrogenase (GAPDH) second intron promoter was amplified with the following primers: 5′-AAT GAA TGG GCA GCC GTT AG-3′ (forward) and 5′-AGC TAG CCT CGC TCC ACCTGA C-3′ (reverse).

Xenograft studies. Two separate xenograft studies were performed independently. Nude mice (*BALB/c nu/nu*; 6-week-old females; CLEA Japan, Inc.) were used for the *in vivo* studies and were cared for in accordance with the recommendations for the Handling of Laboratory Animals for Biomedical Research compiled by the Committee on Safety and Ethical Handling Regulations for Laboratory Animals Experiments, Kinki University. The ethical procedures followed and met the requirements of the United Kingdom Coordinating Committee on Cancer Research guidelines (23). To assess tumorigenicity, suspensions of 1×10^6 H1299/EGFP or H1299/FOXQ1 cells (in 0.1 mL PBS) were s.c. injected into the left or right flanks of nude mice (n = 15), respectively. To evaluate tumor growth, a suspension of 6×10^6 H1299/EGFP, H1299/FOXQ1, H1299/FOXQ1/sh-control, and H1299/FOXQ1/sh-p21 cells (in 0.1 mL PBS) were s.c. inoculated (n = 10) into nude mice. The tumor volume was calculated as length × width^2 × 0.5. The tumor formation was assessed every 2 to 3 d. At the end of the experiment, the mice were sacrificed and the xenografts were resected, fixed in 10% buffered formalin for 6 to 10 h, and processed for histologic analysis.

Immunohistochemical and immunofluorescence staining. The methods used in this section have been previously described (24, 25).

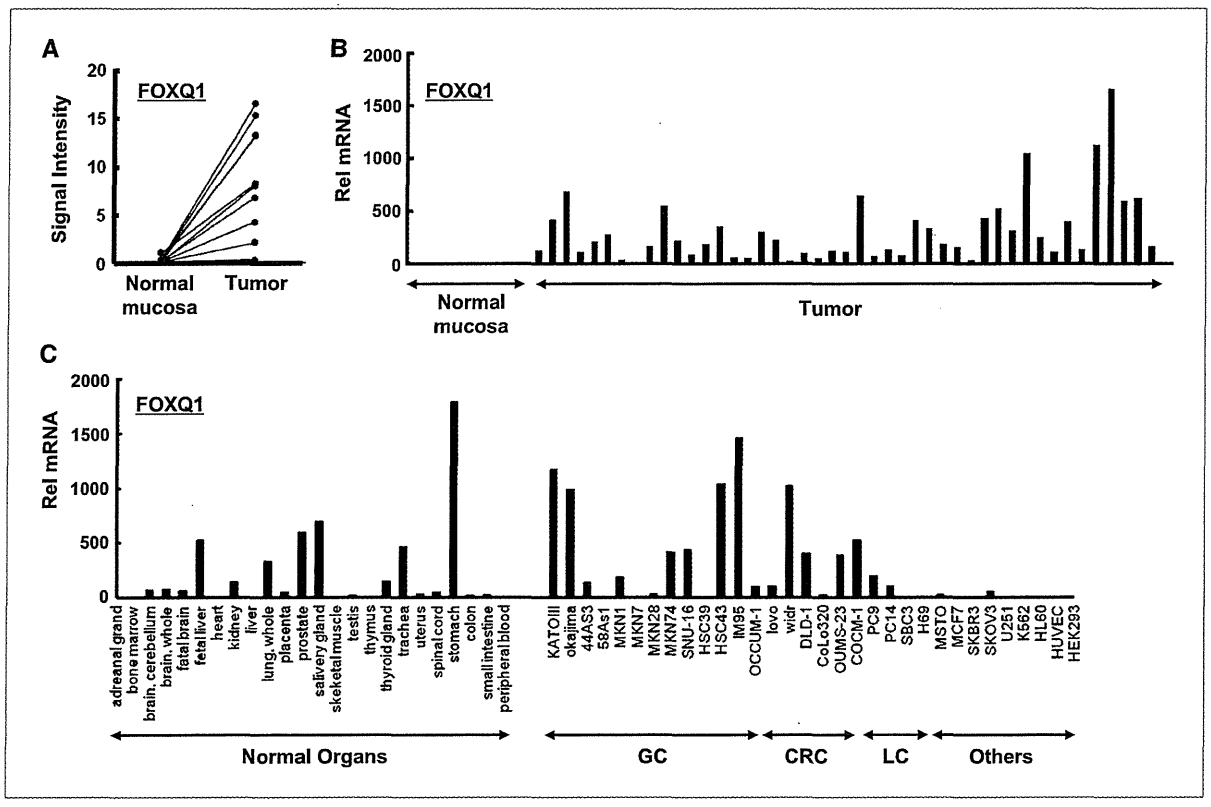

Figure 1. *FOXQ1* expression in CRC. A, mRNA expression of *FOXQ1* obtained from a microarray analysis of 10 CRC and paired normal mucosa specimens. The values indicate the normalized signal intensity. B, the mRNA expression levels of *FOXQ1* were determined using real-time RT-PCR for 10 paired and an additional 36 CRC samples. C, the mRNA expression levels of *FOXQ1* were determined using a real-time RT-PCR analysis of human normal tissue (left) and 30 human cancer cell lines, HEK293, and human umbilical vascular endothelial cell (HUVEC) cell lines (right). GC, gastric cancer; LC, lung cancer; Rel mRNA, normalized mRNA expression levels (*FOXQ1/GAPD* × 10^4).

Downloaded from cancerres.aacrjournals.org on March 20, 2013. © 2010 American Association for Cancer Research.

Published OnlineFirst February 9, 2010; DOI: 10.1158/0008-5472.CAN-09-2161

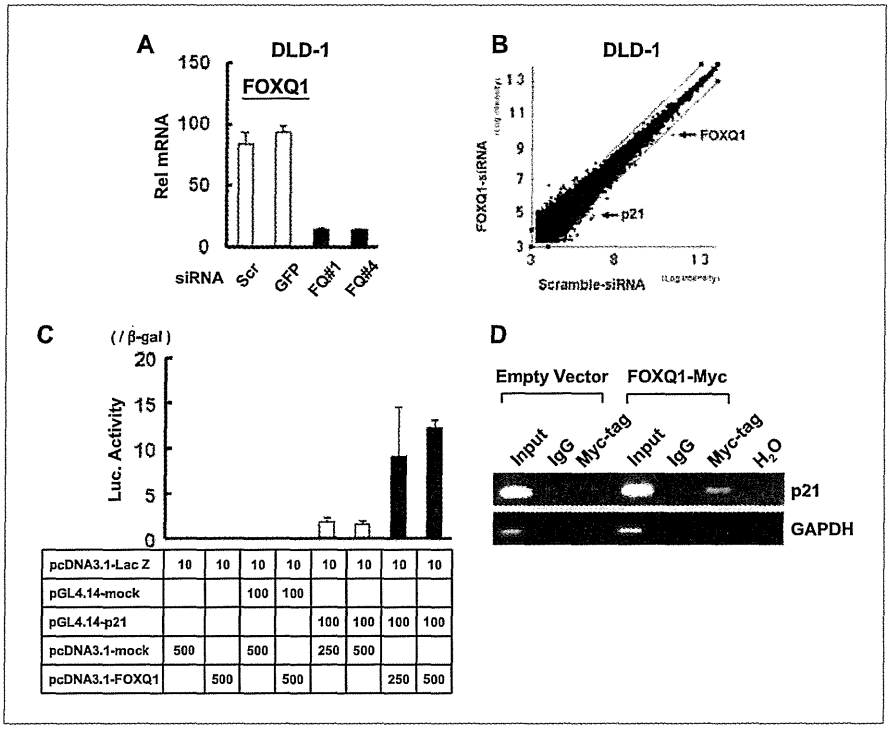

Figure 2. FOXQ directly regulates *p21* transcription. A, FOXQ1-targeting siRNA (FQ#1 and FQ#4) suppressed FOXQ1 expression in DLD-1 cells. The mRNA expression levels of *FOXQ1* were determined using real-time RT-PCR. B, microarray analysis of DLD-1 cells transfected with control-siRNA or FOXQ1-siRNA. The longitudinal axis indicates the mRNA expression of FOXQ1-siRNA transfected cells and the horizontal axis indicates that of control-siRNA. Arrow, FOXQ1 or p21 expression. Each point indicates the normalized and log base 2 transformed microarray data. C, induction of p21 promoter activity by FOXQ1. Luciferase vectors with either an empty or p21 promoter (pGL4.14-mock or pGL4.14-p21) were transiently cotransfected with a mock or FOXQ1 expression plasmid (pcDNA3.1-mock or pcDNA3.1-FOXQ1) expressing β-galactosidase as an internal control. The results were normalized to β-galactosidase activity and are representative of at least three independent experiments. D, ChIP of FOXQ1 on the promoter of *p21*. HEK293 cells were transfected with empty vector (Myc) or Myc-tagged FOXQ1 vector. Agarose gel shows PCR amplification (35 cycles) of the *p21* promoter using inputs (1% of chromatin used for ChIP) or ChIPs as templates. Primers to the *GAPDH* promoter were used as the negative control.

Microarray analysis. The microarray procedure and analysis were performed according to the Affymetrix protocols and BRB Array Tools software, Ver. 3.3.0,[4] developed by Dr. Richard Simon and Dr. Amy Peng, as reported previously (21, 26).

Statistical analysis. The statistical analyses were performed using Microsoft Excel (Microsoft) to calculate the SD and to test for statistically significant differences between the samples using a Student's *t* test. A *P* value of <0.05 was considered statistically significant.

Results

FOXQ1 mRNA was overexpressed in CRCs. A microarray analysis for 10 paired CRC samples identified 30 genes as being significantly upregulated by >10-fold in CRC ($P < 0.001$; Supplementary Table S1). *FOXQ1*, an uncharacterized transcription factor, was upregulated by 28-fold in the CRC specimens (Fig. 1A), exhibiting the fourth highest level of upregulation [after interleukin-8, matrix metalloproteinase-1 (MMP), and MMP-3]. Real-time RT-PCR for the 10 paired samples and an additional 36 CRC samples showed that *FOXQ1* mRNA was markedly overexpressed in the CRC samples but was only expressed at a very low level in noncancerous colonic mucosa ($P < 0.001$; Fig. 1B). The average levels of *FOXQ1* expression were 299 ± 326 and 4.0 ± 5.0 ($\times 10^4$/GAPD), respectively.

FOXQ1 expression in normal tissues and cancer cell lines. To investigate the expression of *FOXQ1*, we analyzed the mRNA expression levels of *FOXQ1* in panels of human normal tissues and cancer cell lines using real-time RT-PCR. High levels of *FOXQ1* expression were observed in the stomach, salivary gland, prostate, trachea, and fetal liver among the 24 normal tissues that were examined (Fig. 1C, left). Relatively weak expression levels were detected in brain-derived tissues, kidney, lung, placenta, and thyroid gland. These results were consistent with those of a previous report (27).

[4] http://linus.nci.nih.gov/BRB-ArrayTools.html

Downloaded from cancerres.aacrjournals.org on March 20, 2013. © 2010 American Association for Cancer Research.

Published OnlineFirst February 9, 2010; DOI: 10.1158/0008-5472.CAN-09-2161

In the cancer cell line panel, the mRNA expression levels of *FOXQ1* were higher in gastric cancer, CRC, and lung cancer cell lines than in the other cancer cell lines, indicating that the expression of *FOXQ1* varies among specific cancers (Fig. 1C, right). Interestingly, the overexpression of *FOXQ1* in CRC arose from normal colonic mucosa with very low expression levels during carcinogenesis.

p21 is a target gene of FOXQ1. To examine the function of FOXQ1 as a transcription factor and to explore its target genes, we performed a microarray analysis using a CRC cell line, DLD-1, transfected with FOXQ1-targeting siRNA or control siRNA. Two sequences of FOXQ1-siRNA, FQ#1 and FQ#4, were used to exclude the off-target effect of siRNA. Real-time RT-PCR showed that both sequences of FOXQ1-siRNA suppressed *FOXQ1* mRNA expression by ~80% in DLD-1 cells (Fig. 2A); thus, FQ#4 was used as the FOXQ1-siRNA in the following experiments. A microarray analysis showed that 19 genes were downregulated by FOXQ1-siRNA (Fig. 2B; Supplementary Table S2); *p21* was the fifth most-downregulated gene. Because p21 is a key regulator of cell cycle and apoptosis, we focused on p21 as a target molecule of FOXQ1.

To confirm the microarray data, p21 downregulation by FOXQ1-siRNA was examined using real-time RT-PCR and a

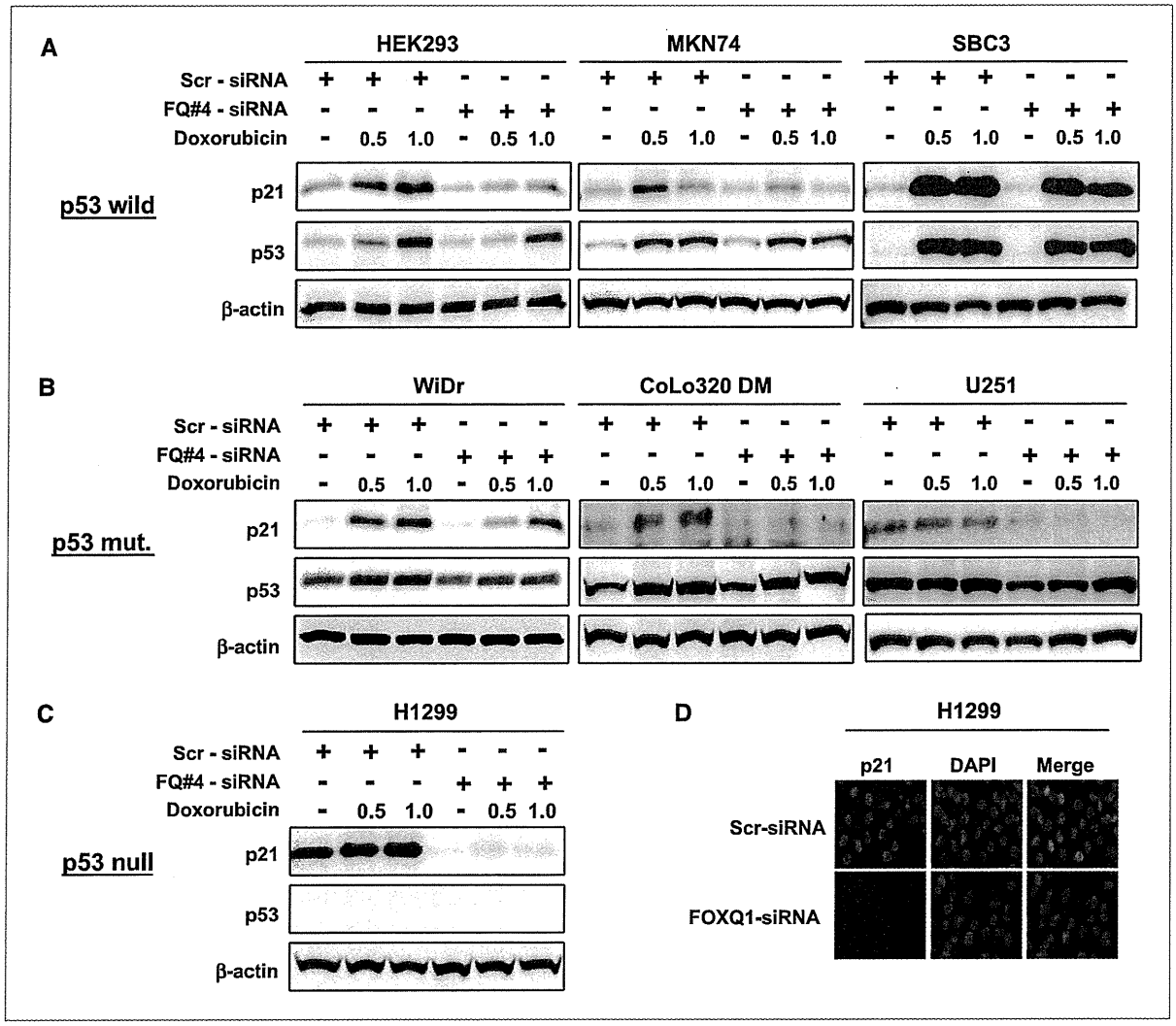

Figure 3. p21 induction by FOXQ1 and p53 status in cancer cells. The seven cell lines were transfected with control-siRNA or FOXQ1-siRNA for 24 h, and the cells were exposed to doxorubicin at a final concentration of 0.5 or 1 μmol/L for a further 24 h to enhance p21 induction. Western blot analyses for p21 and p53 were performed in three p53–wild type cell lines (A), three p53-mutant cell lines (B), and one p53-null cell line (C). The experiment was performed in duplicate. D, immunofluorescence p21 staining and 4′,6-diamidino-2-phenylindole (DAPI) staining for H1299 cells transfected with control-siRNA (top) or FOXQ1-siRNA (bottom) for 48 h. Scr, scramble-siRNA (control); FQ#4, FOXQ1-targeting siRNA. β-Actin was used as an internal control.

Downloaded from cancerres.aacrjournals.org on March 20, 2013. © 2010 American Association for Cancer Research.

Published OnlineFirst February 9, 2010; DOI: 10.1158/0008-5472.CAN-09-2161

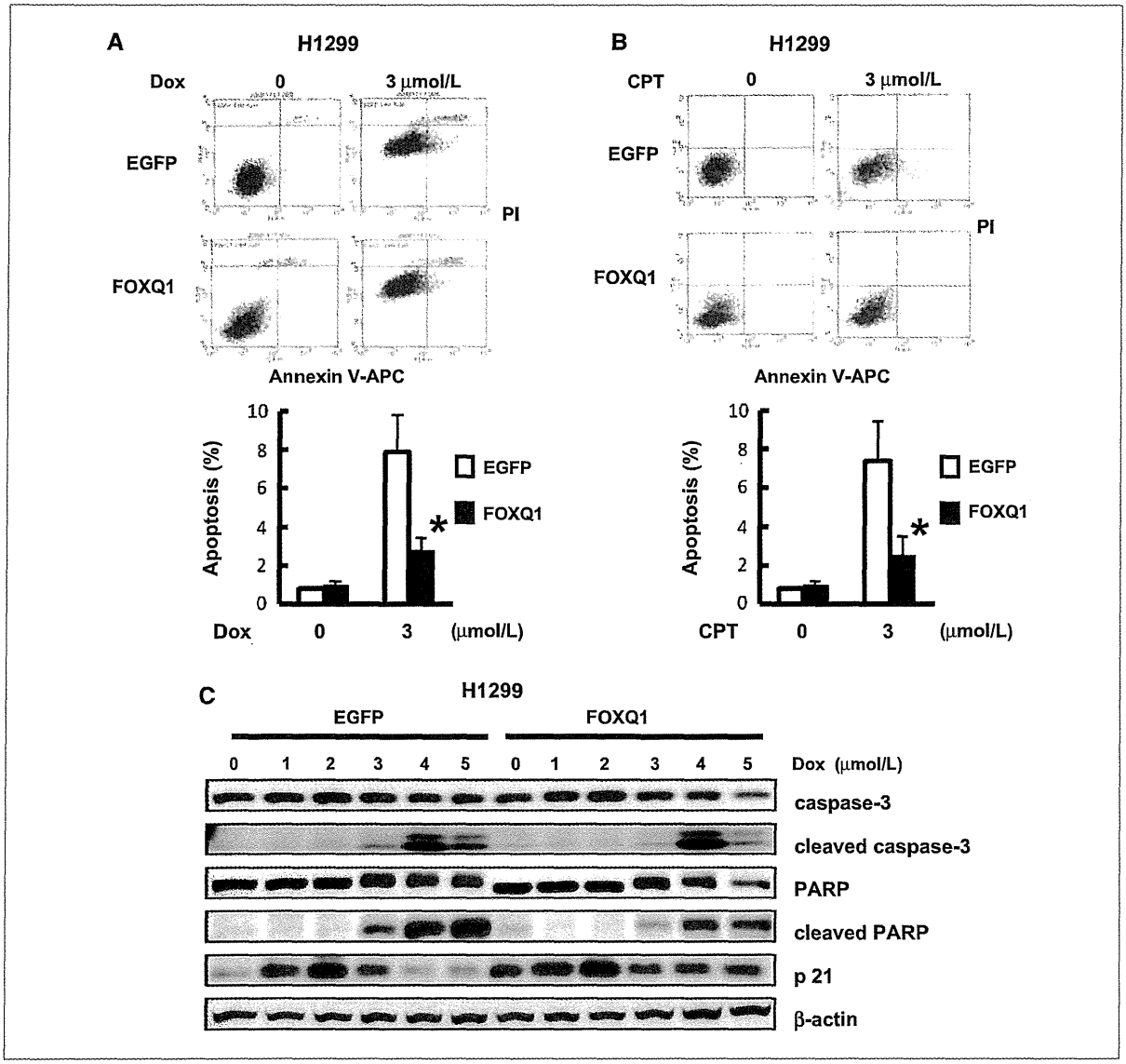

Figure 4. Overexpression of FOXQ1 promotes an antiapoptotic effect. Stable H1299 cell lines expressing EGFP or FOXQ1 (H1299/EGFP, H1299/FOXQ1) were exposed to doxorubicin (A) or camptothecin (B) at a final concentration of 3 μmol/L. Apoptotic cells were detected by Annexin V and propidium iodide (PI) using flow cytometry. C, Western blot analysis for apoptosis-related molecules. EGFP- or FOXQ1-expressing cells were exposed to doxorubicin at the indicated doses (0–5 μmol/L) for 24 h. β-Actin was used as an internal control. Dox, doxorubicin; CPT, camptothecin; EGFP, H1299/EGFP; FOXQ1, H1299/FOXQ1. *, $P < 0.05$.

Western blot analysis in DLD-1 cells. The results indicated that both sequences of FOXQ1-siRNA (FQ#1 and FQ#4) downregulated p21 expression at both the mRNA and protein levels. In addition, we confirmed the downregulation of p21 by FOXQ1-siRNA in other cell lines (WiDr and HEK293), obtaining similar results (Supplementary Fig. S1).

FOXQ1 directly increases the transcription activity of p21. We performed a luciferase reporter assay to determine whether FOXQ1 regulates p21 expression at the transcriptional level. A 2.4-kb section of the p21 promoter region was subcloned into a luciferase vector according to a previously described method (13, 28). The p21 promoter activity was increased by >8-fold when cotransfected with a FOXQ1 expression vector, compared with an empty vector (Fig. 2C). To determine whether FOXQ1 directly binds to p21 promoter, we transfected Myc or Myc-tagged FOXQ1 vectors into HEK293 cells and then conducted ChIP experiments. A segment of the *p21* promoter containing putative FOXQ1 binding site (−2264 to −1971) is precipitated with specific antibody, only if, FOXQ1 was induced (Fig. 2D).

Downloaded from cancerres.aacrjournals.org on March 20, 2013. © 2010 American Association for Cancer Research.

Published OnlineFirst February 9, 2010; DOI: 10.1158/0008-5472.CAN-09-2161

The result indicates that FOXQ1 binds to the *p21* promoter and upregulates p21 transcriptional activity.

p53-independent p21 induction by FOXQ1 in cancer cells. Because p53 is the most important regulatory molecule of p21, we examined the downregulation of p21 by FOXQ1-siRNA in several cell lines with p53–wild type, p53-mutant, or p53-null statuses. These cell lines were transfected with control-siRNA or FOXQ1-siRNA, and p21 induction was enhanced by doxorubicin (29–31). The experiments were performed using three p53–wild type cell lines, three p53-mutation cell lines, and one p53-null cell line (Fig. 3A–C). Without doxorubicin exposure, all seven cell lines showed that p21 expression was downregulated by FOXQ1-siRNA. Notably, with doxorubicin exposure, considerable p21 downregulation by FOXQ1-siRNA was observed in the p53-mutation and p53-null cell lines, compared with in the p53–wild type cell lines. In the p53-null H1299 cell line, FOXQ1-siRNA completely suppressed p21 expression. These results suggest that p21 induction by FOXQ1 is p53 independent. An immunofluorescence study of p21 in H1299 cells also showed that p21 was completely downregulated by FOXQ1-siRNA (Fig. 3D).

Overexpression of FOXQ1 increases p21 expression and exhibits an antiapoptotic effect in cancer cells. Next, we established a stable *FOXQ1*-overexpressing cell line to confirm the induction of p21 expression by FOXQ1 and to detect any changes in the cellular phenotype of the cancer cells. FOXQ1 overexpression induced p21 expression (both mRNA and protein) in HEK293 and CoLo320 cells (Supplementary Fig. S1). Notably, p21 protein expression was markedly induced by >10-fold in the H1299/FOXQ1 cells (Supplementary Fig. S1). These results indicated that FOXQ1 robustly induces p21 expression, consistent with the findings of the siRNA study.

p21 induces an antiapoptotic effect and exerts a protective role against apoptosis induced by DNA damage. To

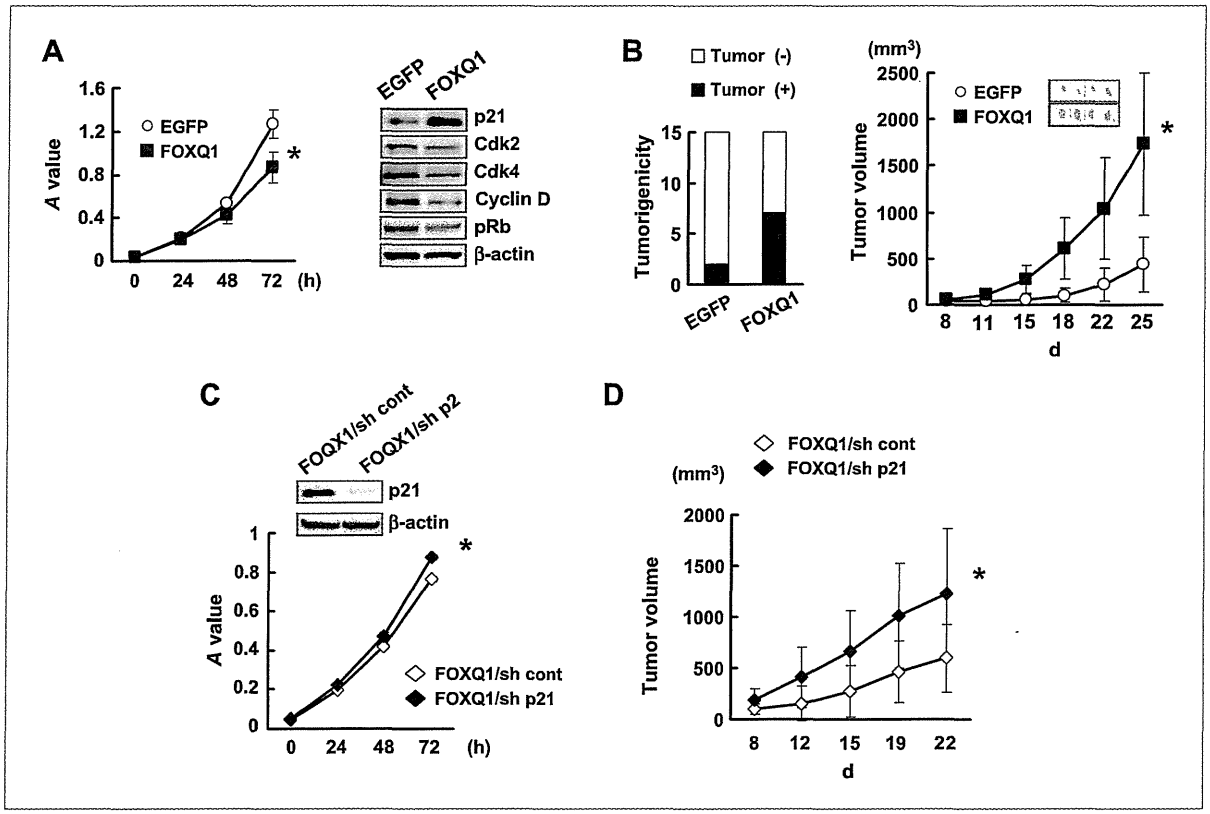

Figure 5. Overexpression of FOXQ1 enhances tumorigenicity and tumor growth *in vivo*. A, cellular growth and immunoblotting analysis of H1299 cell lines stably expressing EGFP or FOXQ1 (H1299/EGFP, H1299/FOXQ1). A total of 2×10^3 cells of each cell line were seeded in 96-well plates and evaluated after 0, 24, 48, and 72 h using MTT assay. Error bars, SD. Protein levels of H1299/EGFP and H1299/FOXQ1 cells were examined by Western blotting using specific antibody to p21, Cdk2, Cdk4, cyclin D, and phosphorylated Rb (pRb) protein. β-Actin was used as an internal control. EGFP, stable EGFP-overexpressing cells; FOXQ1, stable FOXQ1-overexpressing cells. B, H1299/EGFP and H1299/FOXQ1 cells were evaluated for their tumorigenicity *in vivo*. Mice ($n = 15$) were s.c. inoculated with a total of 1×10^6 cells. The numerical data indicate the number of mice. A total of 6×10^6 H1299/EGFP or H1299/FOXQ1 cells were s.c. inoculated into the right flank of each mouse to evaluate the tumor growth *in vivo* ($n = 12$). Representative H&E staining of tumor specimens was also shown. C, stable p21 knockdown or control cells obtained from H1299/FOXQ1 cells (H1299/FOXQ1/sh-control and H1299/FOXQ1/sh-p21) were evaluated for cellular growth and immunoblotting analysis. D, a total of 6×10^6 H1299/FOXQ1/sh-control or H1299/FOXQ1/sh-p21 cells were s.c. inoculated into the right flank of each mouse to evaluate the tumor growth ($n = 10$). *, $P < 0.05$.

Downloaded from cancerres.aacrjournals.org on March 20, 2013. © 2010 American Association for Cancer Research.

Published OnlineFirst February 9, 2010; DOI: 10.1158/0008-5472.CAN-09-2161

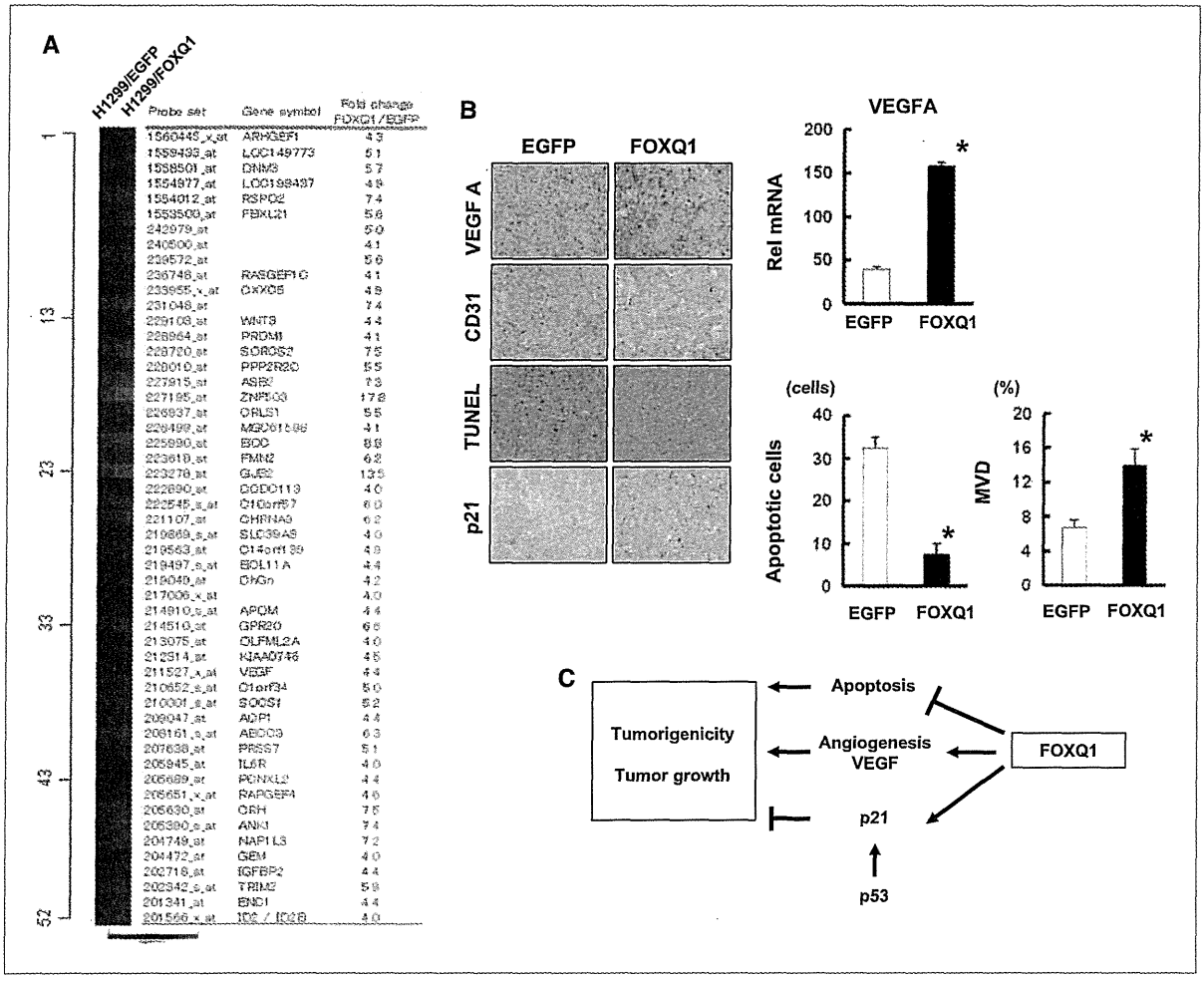

Figure 6. FOXQ1 promotes angiogenic and antiapoptotic effects *in vivo*. A, microarray analysis for H1299/EGFP or H1299/FOXQ1 cells. The upregulated genes over 4-fold by FOXQ1 were shown in the list. B, the mRNA expression levels of *VEGFA* were determined using a real-time RT-PCR analysis. Rel mRNA, normalized mRNA expression levels (*VEGFA/GAPD* × 10^4). VEGF, CD31, TUNEL, and p21 staining of tumor specimens inoculated with H1299/EGFP or H1299/FOXQ1 cells. Microvessel density (MVD) was determined by CD31-positive endothelial cells in tumor specimens using computer-assisted image analysis (Image J software package). C, diagram of a proposed mechanism of FOXQ1 for tumorigenicity and tumor growth. *, $P < 0.05$.

elucidate the role of apoptosis induced by FOXQ1 in cancer cells, we examined the apoptotic effect in H1299/EGFP and H1299/FOXQ1 cells using anticancer drugs. The overexpression of FOXQ1 inhibited the apoptosis induced by doxorubicin (H1299/EGFP: 7.9 ± 1.9%, H1299/FOXQ1: 2.7 ± 0.7%; Fig. 4A). Similarly, camptothecin-induced apoptosis was also inhibited in FOXQ1-overexpressing cells (H1299/EGFP: 7.4 ± 2.1%, H1299/FOXQ1: 2.5 ± 1.0%; Fig. 4B). Western blotting revealed that FOXQ1 overexpression decreased the levels of cleaved caspase-3 and cleaved PARP induced by doxorubicin (Fig. 4C). These results are consistent with those obtained using flow cytometry.

***Overexpression of FOXQ1 decreases cellular proliferation but enhances tumorigenicity and tumor growth* in vivo.** Stable H1299/FOXQ1 cells showed decreased cellular proliferation compared with control cells *in vitro* (Fig. 5A). Expressions of Cdk4, cyclin D1, and Cdk2 were decreased by FOXQ1 expression in H1299/FOXQ1 cells and resulted in a decrease of phosphorylated Rb expression (Fig. 5A). To examine the biological functions of FOXQ1 overexpression *in vivo*, we evaluated tumorigenicity and tumor growth using H1299/EGFP or H1299/FOXQ1 cells. H1299/FOXQ1 cells exhibited a significantly elevated level of tumorigenesis *in vivo* (GFP 2/15, FOXQ1 7/15, $P < 0.05$; Fig. 5B). In addition, the tumor volume was markedly larger in H1299/FOXQ1 cells than in H1299/EGFP cells (EGFP: 437 ± 301, FOXQ1: 1735 ± 769 mm^3, $P < 0.001$; Fig. 5B) on day 25.

***p21 does not contribute to FOXQ1-mediated tumor growth* in vivo.** Because emerging evidence has indicated that p21 may have dual functions with regard to tumor

Downloaded from cancerres.aacrjournals.org on March 20, 2013. © 2010 American Association for Cancer Research.

Published OnlineFirst February 9, 2010; DOI: 10.1158/0008-5472.CAN-09-2161

progression and the suppression of cancer cells (32, 33), the shRNA targeting p21 or shRNA control viral vectors were further introduced into the H1299/FOXQ1 cells to elucidate the involvement of p21 in increased FOXQ1-mediated tumorigenicity and tumor growth *in vivo*. Stable H1299/FOXQ1/sh-p21 cells were slightly increased in cellular proliferation *in vitro* (Fig. 5C). In addition, tumor growth of H1299/FOXQ1/sh-p21 cells was increased compared with control cells *in vivo* (Fig. 5D). The results clearly indicate that p21 has negative roles for cellular proliferation and tumor growth in FOXQ1-overexpressing cells, suggesting that p21 does not contribute to FOXQ1-mediated tumor growth in FOXQ1-overexpressing cells *in vivo*.

***Overexpression of FOXQ1 promotes angiogenesis and antiapoptosis* in vivo.** To gain an insight into the mechanism by which FOXQ1 enhances tumor growth *in vivo*, we performed the microarray analysis on H1299/EGFP and H1299/FOXQ1 cells. Fifty-two genes were upregulated over 4-fold by overexpression of FOXQ1 including several genes that have positive roles for tumor growth, such as *VEGFA, WNT3A, RSPO2,* and *BCL11A* (Fig. 6A). Overexpression of FOXQ1 upregulated the *VEGFA* expression for 4.4-fold, suggesting the possibility of enhanced angiogenesis. Real-time RT-PCR for these cells and vascular endothelial growth factor (VEGF) staining of tumor specimens confirmed the result (Fig. 6B). Furthermore, CD31 staining of the tumor specimens showed that FOXQ1 overexpression significantly increased the angiogenesis *in vivo*.

Terminal deoxynucleotidyl transferase-mediated dUTP nick end labeling (TUNEL) and p21 immunostaining of the tumor specimens showed that p21 expression was increased and apoptosis was inhibited in H1299/FOXQ1 cells (Fig. 6B). These results strongly suggest that FOXQ1 promotes tumorigenicity and tumor growth with its angiogenic and antiapoptotic properties *in vivo* (Fig. 6C).

Discussion

FOX transcription factors are an evolutionarily conserved superfamily that control a wide spectrum of biological processes. Several Fox gene family members are involved in the etiology of cancer. Only the FOXO family has been regarded as *bona fide* tumor suppressors that promote apoptosis and cell cycle arrest at G_1 (34, 35). The loss of FOXO function observed in alveolar rhabdomyosarcoma through chromosomal translocation was first identified in relation to cancer. Many target genes of FOXO have been reported to date, including p21, cyclin D, Bim, TRAIL, and ER-α (36). On the other hand, the overexpression of FOXM is observed in head and neck cancer, breast cancer, and cervical cancer, and it enhances proliferation and tumor growth *in vitro* (37), suggesting that *FOXM* may be an oncogene. Although the available evidence is not conclusive, FOXP, FOXC, and FOXA have been linked to tumorigenesis and progression of certain cancers (36). Thus, the FOX family is thought to act as either an oncogene or a tumor suppressor. In the present study, we showed that the overexpression of FOXQ1 played a tumor-promoting role in CRC.

The p21 promoter region contains several definitive DNA regulatory elements, such as the p53-binding domain, E-box, Smad binding element, and TGF-β response elements. In the case of the other FOX family member FOXO, a recent report showed that the p21 promoter contains a consensus forkhead binding element (GGATCC) immediately upstream of the first Smad binding element and that the FOXO and Smad complexes activate p21 expression, whereas the FOXG1 protein binds to FOXO and blocks p21 induction (38). On the other hand, the consensus binding sequence (5′-NA(A/T)TGTTTA(G/T)(A/T)T-3′) has been defined for human FOXQ1 (4). The p21 promoter region contains several putative FOXQ1 binding sites according to its consensus binding sequence. Indeed, we have shown that FOXQ1 binds to a segment of the p21 promoter, indicating that FOXQ1 directly transactivates the p21 gene expression.

The initial descriptions of p21 were thought to indicate a tumor suppressor–like role, and p21 was almost solely regarded as a modulator with the principal function of inhibiting a cyclin-dependent kinase activity and, hence, cell cycle progression, because it was originally identified as a mediator of p53-induced growth arrest. However, emerging evidence has indicated that p21 may have dual functions with regard to tumor progression and the suppression of cancer cells, with examples of other genes with dual functions including TGF-β, Notch, Runx3, E2F, and p21 (32). Besides its growth inhibitory role, p21 is known to have a positive effect on cell proliferation (39–41). A more recent study on leukemic stem cells showed a p21-dependent cellular response that leads to reversible cell cycle arrest and DNA repair; such data clearly illustrate the oncogenic potential of p21 (33). We have shown that p21 has negative roles for tumor growth using FOXQ1-overexpressing cells with knockdown of p21 (Fig. 5D).

Recently, accumulating evidence has shown that FOX transcriptional factors are involved in VEGF regulation and angiogenesis. For example, forkhead has exhibited a positive role in mediating induction of VEGF (42–44). In the present study, we identified *VEGFA* as a candidate target gene of FOXQ1 by microarray analysis and showed that FOXQ1 increased angiogenesis *in vivo*. Interestingly, although overexpression of FOXQ1 decreases cellular proliferation *in vitro*, it enhances tumorigenicity and tumor growth *in vivo*. We consider that this discrepancy can be explained by these angiogenic and antiapoptotic effects of FOXQ1 contribute to enhanced tumor growth *in vivo*, although p21 negatively functions.

We showed that the overexpression of FOXQ1 inhibited doxorubicin-induced and camptothecin-induced apoptosis in p53-inactivated cancer cells. Therefore, we speculated that FOXQ1 might be a new determinant factor of resistance to drug-induced apoptosis and might represent a poor prognostic factor for CRC patients.

In conclusion, FOXQ1 is markedly overexpressed in CRC and enhances tumorigenicity and tumor growth *in vivo*. We have elucidated a biological function of FOXQ1, which directly upregulates p21 transcription and promotes angiogenesis and antiapoptosis. Our findings support FOXQ1

Downloaded from cancerres.aacrjournals.org on March 20, 2013. © 2010 American Association for Cancer Research.